
Doctoral Dissertations

Student Theses and Dissertations

1969

A crystallization study of a tetrasilicic fluormica glass

William H. Daniels

Follow this and additional works at: https://scholarsmine.mst.edu/doctoral_dissertations



Part of the [Ceramic Materials Commons](#)

Department: **Materials Science and Engineering**

Recommended Citation

Daniels, William H., "A crystallization study of a tetrasilicic fluormica glass" (1969). *Doctoral Dissertations*. 2101.

https://scholarsmine.mst.edu/doctoral_dissertations/2101

This thesis is brought to you by Scholars' Mine, a service of the Missouri S&T Library and Learning Resources. This work is protected by U. S. Copyright Law. Unauthorized use including reproduction for redistribution requires the permission of the copyright holder. For more information, please contact scholarsmine@mst.edu.

A CRYSTALLIZATION STUDY OF A TETRASILICIC FLUORMICA GLASS

by

WILLIAM H. DANIELS

A DISSERTATION

Presented to the Faculty of the Graduate School of the
UNIVERSITY OF MISSOURI-ROLLA

In Partial Fulfillment of the Requirements for the Degree

DOCTOR OF PHILOSOPHY

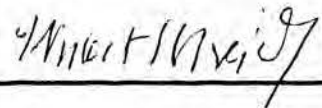
in

CERAMIC ENGINEERING

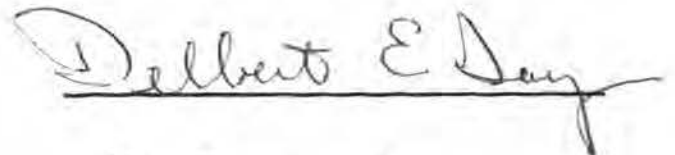
1969



Advisor











Abstract

The transformation of a synthetic mica composition $K_2Mg_5Si_8O_{20}F_4$ from amorphous to crystalline structure was studied isothermally at selected temperatures from 560°C to 1150°C. Thermal changes associated with the transformation were followed by differential thermal analysis techniques. Structural changes promoted by the isothermal treatments were observed by density measurements, Debye-Scherrer X-ray diffraction techniques, electron replication microscopy, and electron scanning microscopy.

Isothermal treatment at 560°C for 9 hours produces structural ordering in quenched $K_2Mg_5Si_8O_{20}F_4$ glass. Fluorine exerts a significant influence on the transformation temperature; decreasing amounts of fluorine producing increasing transformation temperatures. The crystallizing phase rapidly attains a limiting particle size and morphology at temperatures in the 600°C region. Treatments of quenched $K_2Mg_5Si_8O_{20}F_4$ glass at 900°C and above promotes a change from spherulitic to blocky crystal habit, accompanied by a more complete development of mica structure during growth.

Acknowledgment

The author wishes to express his sincere appreciation to the members of his graduate advisory committee, Dr. R. E. Moore, Dr. D. E. Day, Dr. C. E. Antle, Dr. W. P. Tappmeyer, and Dr. O. H. Hill, for their support and guidance.

The writer is also indebted to the many members of the staff, especially Dr. N. J. Kreidl and Dr. G. Lewis for assistance, suggestions and inspiration.

The electron scanning microscopy work was made possible through the cooperation of Monsanto Company, St. Louis, Missouri. The assistance of Dr. J. D. Fairing and Dr. R. Schierding of that organization is deeply appreciated.

The electron microscopy work performed at Union Carbide Corporation in Kokomo, Indiana was obtained through the cooperation of several staff members, whose assistance is gratefully acknowledged.

The financial support of the National Science Foundation which made this work possible is deeply appreciated.

TABLE OF CONTENTS

	<u>Page</u>
Abstract	ii
Acknowledgment	iii
List of Figures	vi
List of Tables	viii
I. Introduction	1
II. A Review of the Literature	4
A. The Crystal Structure of Mica	4
B. Glass Crystallization	8
C. Glass-Ceramic Fabrication of Fluormicas	11
D. Kinetic Studies of Glass Crystallization	13
1. Linear Growth Studies	13
2. Volume Transformation	16
III. Experimental Procedure	19
A. Sample Preparation	19
1. Raw Materials	19
2. Melting and Forming	19
3. Sample Selection	22
4. Sample Treatment	22
B. Differential Thermal Analysis	23
C. Density Measurements	23
D. X-ray Diffraction	24
E. Microscopic Examination	25
IV. Experimental Results	26
A. Chemical Analysis	2

	<u>Page</u>
B. Differential Thermal Analysis	26
C. Density Measurements	29
D. X-Ray Diffraction	33
E. Electron Microscopy	39
F. Electron Scanning Microscopy	45
G. Phase Transformations	45
V. Discussion of Results	54
A. Chemical Analysis	54
B. Structural Transformations	55
1. Early Stages of the Structural Transformations	55
2. Final Stages of the Transformation	58
VI. A Proposed Mechanism for Crystallization of $K_2Mg_5Si_8O_{20}F_4$ Glass	62
VII. Conclusions	65
Bibliography	66
Vita	69

LIST OF FIGURES

<u>Figure Number</u>	<u>Page</u>
1. Schematic Structure of Fluormica $K_2Mg_5Si_8O_{20}F_4$.	6
2. Typical Differential Thermal Analysis Curve for As-quenched $K_2Mg_5Si_8O_{20}F_4$ Glass	28
3. Differential Thermal Analysis of $K_2Mg_5Si_8O_{20}F_4$ Glass Pre-heated at 600°C for Indicated Time Periods	31
4. Differential Thermal Analysis of $K_2Mg_5Si_8O_{20}F_4$ Glass Pre-heated at 620°C and 640°C.	32
5. Density vs. Heat Treatment Time at 560° to 625°C for $K_2Mg_5Si_8O_{20}F_4$ Glass	34
6. Density vs. Heat Treatment Time at 1070° to 1150°C for $K_2Mg_5Si_8O_{20}F_4$ Glass	35
7. X-ray Diffraction Patterns of $K_2Mg_5Si_8O_{20}F_4$ Glass - As-quenched and Treated Isothermally at 560°C.	36
8. X-ray Diffraction Patterns of $K_2Mg_5Si_8O_{20}F_4$ Glass Heat Treated Isothermally at 580°C.	37
9. X-ray Diffraction Patterns of $K_2Mg_5Si_8O_{20}F_4$ Glass Heat Treated Isothermally at 600°C and 625°C.	38
10. X-ray Diffraction Patterns of $K_2Mg_5Si_8O_{20}F_4$ Glass Heat Treated at 700°C, 800°C, 900°C, and 1000°C.	40
11. X-ray Diffraction Patterns of $K_2Mg_5Si_8O_{20}F_4$ Glass Heat Treated at 1100°C, 1125°C, 1150°C and $K_2Mg_5Si_8O_{20}F_4$ Standard Pattern	41
12. Electron Micrographs of As-quenched $K_2Mg_5Si_8O_{20}F_4$ Glass and 560°C Isothermal Heat Treatments	43
13. Electron Micrographs of $K_2Mg_5Si_8O_{20}F_4$ Glass Heat Treatments at 600°C, 800°C, and 900°C.	44
14. Electron Scanning Micrographs of $K_2Mg_5Si_8O_{20}F_4$ Glass Heat Treated Isothermally at 1100°C.	46
15. Electron Scanning Micrographs of $K_2Mg_5Si_8O_{20}F_4$ Glass Heat Treated Isothermally at 1125°C.	47

<u>Figure Number</u>	<u>Page</u>
16. Electron Scanning Micrographs of $K_2Mg_5Si_8O_{20}F_4$ Glass Heat Treated Isothermally at $1150^\circ C$. . .	48
17. Temperature Dependence of Transformation Rate for $K_2Mg_5Si_8O_{20}F_4$ Glass in the $600^\circ C$ Region	50
18. Particle Size of $K_2Mg_5Si_8O_{20}F_4$ Crystals Growing from Glass vs. Heating Time at Temperatures from $1070^\circ C$ to $1150^\circ C$	52
19. Crystal Growth Rate of Synthetic Mica $K_2Mg_5Si_8O_{20}F_4$ from a Glass of the Same Composition	53

LIST OF TABLES

<u>Table Number</u>		<u>Page</u>
I.	Batch Compositions for $K_2Mg_5Si_8O_{20}F_4$ Glass . . .	20
II.	Chemical Analyses of Glass Samples	27
III.	Variation of Exothermic Peak Temperature with Fluorine Content	30
IV.	Results of Analysis for Largest Particle from Electron Scanning Micrographs	51

I. INTRODUCTION

The synthesis of mica compounds has been intensively researched by several investigators over the past three decades. Significant research programs on synthetic mica fabrication have been conducted in Russia, Germany, Japan, and the United States with varied success. Initially the motivation for these investigations was a desire for a suitable substitute for the strategic mica mineral. However, more recently interest in fluormica compounds as new engineering materials has arisen, stimulated by the large number of isomorphic substitutions creating the possibility of designing materials with desired properties over wide ranges.

A variety of methods have been employed to synthesize fluormica compounds including melt crystallization, solid state reaction, hot pressing, and glass-ceramic fabrication techniques. These methods usually yield a polycrystalline ceramic material, although recently single crystals of fluormica have been fabricated by a sophisticated melt crystallization process.⁽¹⁾ Only one of these techniques, glass-ceramic fabrication, is treated in this investigation.

This study is a continuation of a series of investigations on the physical characteristics of the tetrasilicic fluormica compound $K_2Mg_5Si_8O_{20}F_4$ conducted at the

University of Missouri-Rolla. Previous work includes development of the composition and fabrication techniques,⁽²⁾ determination of dielectric behavior,⁽³⁾ and evaluation of the elastic and anelastic constants⁽⁴⁾ of this material. The results of these investigations indicate that a structural transformation occurs at temperatures as low as 600°C during heating of the quenched glass. However, the synthetic mica crystals do not appear until temperatures in the range from 1000°C to the melting point are attained.

The transformation in the region of 600°C is strikingly evident in dynamic elastic modulus, effects on mechanical damping, and thermal expansion measurements.^(3, 4) X-ray diffraction studies on the glass, heated to temperatures slightly above this transformation point, revealed a series of broad peaks shifted somewhat from expected mica d-spacings. As heat treatment temperatures increased toward 1000°C these peaks increased in sharpness and intensity, eventually giving rise to diffraction patterns of the tetrasilicic fluormica after heat treatment for several hours to a few days in the temperature range 1000°C to 1150°C.

Based upon these results this investigation was designed to gain a better understanding of the structural transformations encountered during the crystallization of the tetrasilicic fluormica $K_2Mg_5Si_8O_{20}F_4$ from a quenched

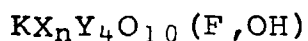
glass. Major objectives were to establish the nature of the phases resulting from the transformations, the temperature at which the initial transformation occurs, and the kinetic behavior of the transformation. Experimental techniques employed included electron microscopy, X-ray diffraction, density determinations, electron scanning microscopy, and differential thermal analysis.

II. A REVIEW OF THE LITERATURE

A. The Crystal Structure of Mica

The complex structure of mica compounds has intrigued mineralogists and crystal chemists for over fifty years. While this study is not of a mineralogical nature, a discussion of the crystalline structure and structural classifications of mica materials which have developed is helpful in understanding the nature of the glass-fluormica transformation.

Several classification systems for mica compounds based upon molecular composition and crystal structure are proposed in the literature. One of the most general structural formulas is that of the form given by Pauling:⁽⁵⁾



where

$$2 \leq n \leq 3$$

X represents cations of coordination number six

Y represents cations of coordination number four, chiefly Si^{+4} and Al^{+3} .

Applying this formula to synthetic fluormica compounds yields a general formula $ZX_nY_4O_{10}F_2$, where Z is used to denote a cation of coordination number twelve, usually potassium as noted by Pauling, but possibly calcium or

sodium.

Winchell⁽⁶⁾ classifies micas into two systems, heptaphyllite and octaphyllite, indicating either seven or eight atoms per molecule (exclusive of O and F) and corresponding to the extreme values of Pauling's subscript n . These systems are of interest later in the discussion of fluormica compounds studies here.

The structure of synthetic mica is shown schematically in Figure 1.⁽⁷⁾ Basically it consists of two sheets of YO_4 tetrahedra with their vertices pointing inward. These tetrahedra are linked in one plane by sharing the three oxygen atoms which form the base of each tetrahedron, each atom being shared by two tetrahedra. Continuous extension of this linkage creates a hexagonal network within each tetrahedrally coordinated plane. The two tetrahedral sheets are strongly bonded together by cations of type X which are in sixfold or octahedral coordination. The fluorine ions, although lying in the plane of the apical oxygen ions, are actually bonded only to the X type cations. Thus the anions forming the octahedral site are two fluorine and four oxygen ions. The Z cations in twelvefold coordination perform the function of bonding adjacent double sheets together. The cleavage plane so characteristic of mica minerals lies between sets of the double sheets.

The cations in tetrahedral coordination are usually either silicon ions or a combination of silicon and

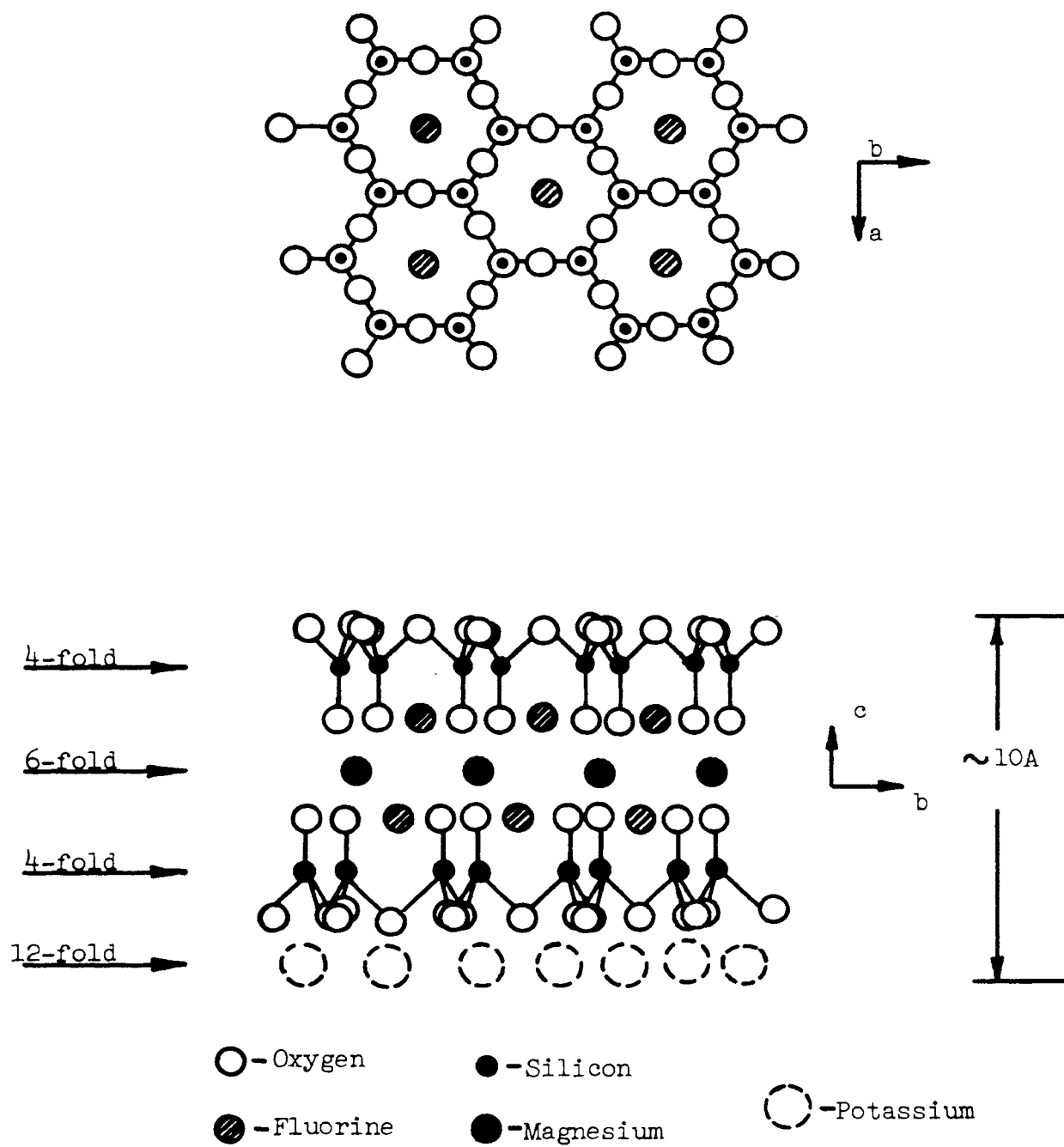


Figure 1. Schematic Structure of Fluormica $K_2Mg_5Si_8O_{20}F_4$

aluminum ions. Micas containing only silicon in the tetrahedral sites are called tetrasilicic; those containing an average silicon to aluminum ratio of 3:1 in fourfold coordination, trisilicic; and those mica compounds with equal numbers of silicon and aluminum ions in YO_4 coordination, disilicic.

In the octahedral sites formed by two fluorine and four oxygen ions are found cations having ionic radii of from 0.6 to 0.9 $\overset{\circ}{\text{A}}$. Those cations most often found in these positions are Mg^{+2} , Al^{+3} , Fe^{+3} , Mn^{+2} , Mn^{+3} , Ti^{+4} , and Li^{+} . Two distinct groups of mica compounds, as determined by the number of filled octahedral positions are known to exist. Those having 2/3 of the available octahedral sites filled are called dioctahedral, and those having all octahedral positions filled, trioctahedral. These groups would correspond to Winchell's heptaphyllite and octaphyllite series.

Considering the structure of the fluormica, $K_2Mg_5Si_8O_{20}F_4$, studied herein, in light of the preceding discussion, it is noteworthy that this molecule is tetrasilicic, but falls into neither the octaphyllite or heptaphyllite series. Although this fluormica has no known natural mica analog, Siefert and Schreyer⁽⁸⁾ recently reported the synthesis of the compound $KMg_{2.5}Si_4O_{10}(OH)_2$ by hydrothermal techniques. They emphasize the theoretical importance of this compound for the crystal chemistry

of the whole mica system. Having 2.5 octahedral sites filled, the phase represents an intermediate member between the dioctahedral and trioctahedral series, which have generally been considered as independent groups. Preliminary experiments on this hydrothermally formed compound suggest that it is linked to other micas by simple substitutions. Results of this work indicate that the new phase may form solid solutions with trioctahedral pure phlogopite, $\text{KMg}_3[\text{Si}_3\text{AlO}_{10}](\text{OH})_2$.

A meager amount of physical property data is reported in the literature for the compound $\text{K}_2\text{Mg}_5\text{Si}_8\text{O}_{20}\text{F}_4$. In addition to data from work done at the University of Missouri-Rolla cited previously, (2,3,4) Alley and Shell (9) report the melting point of the compound $\text{K}_2\text{Mg}_5\text{Si}_8\text{O}_x\text{F}_{4.5}$ as 1176°C , and Hatch, et al (10) report the unit cell dimensions, $a_0 = 5.218\text{A}$, $b_0 = 9.160\text{A}$, $c_0 = 20.105\text{A}$, with a β value of 95° , and a density of 2.835 gms/cm^3 for the compound of ideal composition $\text{K}_2\text{Mg}_5\text{Si}_8\text{O}_{20}\text{F}_4$.

B. Glass Crystallization

Controlled crystallization of glass resulting in non-porous, fine-grained, polycrystalline materials may occur through a nucleation and growth mechanism or through a liquid-liquid unmixing followed by crystal formation. (11) Classical nucleation theory for condensed systems describes nuclei formation as either homogeneous or heterogeneous,

the latter indicating the preferential occurrence of nuclei at special sites or singularities, as opposed to intrinsic or homogeneous nucleation. ⁽¹¹⁾ Phase separation in glasses by a liquid-liquid unmixing or spinodal mechanism involves the spontaneous decomposition of an unstable homogeneous phase into two related phases differing only in chemical composition. Cahn and Charles ⁽¹²⁾ point out that phases formed by this mechanism may or may not be equilibrium phases.

Stookey and Mauer ⁽¹³⁾ discuss the uniqueness of glass arising from the enormous viscosity change from liquid to brittle solid upon cooling. An important consequence of this behavior is that high temperature equilibrium states or structures are frozen into the quenched glass. This structure freezing phenomenon is the key factor making possible the unique control of crystallization inherent in glass ceramics. Using free energy-temperature diagrams Roy ⁽¹⁴⁾ discusses several metastable equilibrium states which may be encountered in quenched glasses and describes distinct steps which can be recognized in the isothermal crystallization of such glasses.

Once a quenched glass is obtained, crystallization through subsequent thermal treatment is influenced by the "frozen in" structural states and relates to the free energy-composition relationships for the specific glass in question. If the amorphous phase is unstable to local

compositional fluctuations as described by Cahn,⁽¹⁵⁾ spontaneous separation into two phases occurs; the only barrier to such a process is a diffusional one. In systems where the amorphous phase is metastable to local compositional fluctuations, a nucleus cannot form without an increase of free energy for the system and hence constitutes a barrier to nucleation.⁽¹²⁾

LaMer⁽¹⁶⁾ discusses the process involved in forming a new stable phase within a metastable mother phase. The two factors which control the magnitude of the energy barrier to nucleation are the energy per unit area of surface between the two phases and the magnitude of the free energy change per unit volume in transforming from one phase to another. The effect of nucleation catalysts is to lower the surface energy term, thereby lowering the magnitude of the nucleation barrier.⁽¹²⁾

Upon formation of a critical nucleus the velocity of crystal growth becomes the controlling factor in the amorphous to crystalline transformation. In a comprehensive review of glass crystallization theory and practice, Emrich⁽¹⁷⁾ lists several factors which can influence crystal growth rates including viscosity of the glass, concentration of crystallizing elements, heat transfer rate to or from the region of crystallization, and rate of diffusion to and from the region of crystallization. However, Stookey and Maurer⁽¹²⁾ maintain that in a glass which crystallizes to

its own composition, such as that in the current investigation, growth is primarily limited by reactions occurring at the crystal-glass interface.

C. Glass-Ceramic Fabrication of Fluormicas

Hatch, et al⁽¹⁰⁾ selected the tetrasilicic fluormica $K_2Mg_5Si_8O_{20}F_4$ for fusion casting experiments because the high silica content results in greatly increased viscosity over fluormica compositions containing alumina. Batches fused in fireclay crucibles at 1300 to 1450°C were cast in graphite or iron molds at temperatures from ambient to 800°C. Attempts also were made to quench this melt by solidifying in a platinum dish chilled by air or water. In either case the product was glassy and brittle, although it was successfully devitrified by reheating slowly to 1000°C. These investigators suggest that successful fabrication of mica glasses should be possible through controlled chilling of the melt in small shapes or sheets up to one inch thick.

Tuzzeo⁽²⁾ synthesized the tetrasilicic fluormica $K_2Mg_5Si_8O_{20}F_4$ by glass-ceramic fabrication in the form of bubbles, disks, and rods. Isothermal treatments at selected temperatures from 620 to 1160°C produced materials with varying crystalline content. Attempts were made to correlate density changes, dielectric loss, and dielectric constant values of the glass-mica material to mica content.

In a study of the dielectric behavior of this same

tetrasilicic fluormica Schumacher⁽³⁾ reported development of an intermediate "pseudocrystalline" phase prior to devitrification of the mica glass to the final crystalline product. This phase formed at temperatures slightly above 600°C and possessed some ordering of the crystalline state as indicated by X-ray diffraction patterns. The crystalline mica was thought to grow from the "pseudocrystalline" phase, with complete development of the mica attained after heat treatments at 900 and 1000°C for 3 hours as assessed by density measurements. Heat treatment at 1150°C for six days produced particles up to 100 microns in the longest direction.

Ainsworth⁽⁴⁾ determined elastic and anelastic properties of $K_2Mg_5Si_8O_{20}F_4$ in addition to determination of density changes, weight loss, and thermal expansion encountered during heat treatment of the glass. The elastic and anelastic constants decreased gradually from 600 to 1000°C indicative of progressively increased structural ordering. Heat treatments above 1000°C produced significant decreases in elastic constants and similar increases in damping. This behavior was attributed to increasing mica crystal growth. Elastic modulus, log decrement and thermal expansion measurements indicate a change from amorphous to ordered structure at 600°C.

Chen⁽¹⁸⁾ studied the crystallization kinetics of a synthetic mica glass, the exact composition of which was not disclosed, but reported to be close to fluorphlogopite

$K_2Mg_6Al_2Si_6O_{20}F_4$ and containing some B_2O_3 additions. The crystallization of this synthetic mica material was described as a two stage process; an intermediate phase, termed as pseudocrystalline, existed from 700 to 860°C with the mica structure forming at higher temperatures within the intermediate phase. The intermediate phase, as shown in electron micrographs, exhibited plate-like structure but no distinct grain boundaries were apparent at points where adjacent regions grew to impingement. X-ray diffraction studies on a series of specimens indicate that treatment at 1000°C produced a pattern matching that of synthetic fluorphlogopite mica. Specimens treated at 720 and 850°C exhibited principal diffraction lines matching the mica pattern, while treatment at 700°C produced only a glass halo. In addition specimens treated at 720, 850, and 1000°C exhibited a broad band of d-spacings over the range 2.41 to 2.50 Å, which was related to the pseudocrystalline phase.

D. Kinetic Studies of Glass Crystallization

1. Linear Growth Studies

Most of the kinetic studies of glass crystallization reported in the literature are concerned with the rate of advance of a crystallization layer from a stable nucleus. Rindone⁽¹⁹⁾ determined the rate of crystallization of $Li_2O \cdot 2SiO_2$ from a $Li_2O \cdot 4SiO_2$ glass as a function of platinum concentration at 600 and 650°C. Noting that rate

processes, such as those involved in nucleation and crystallization, have been interpreted on the basis that an activation energy is required for each of the steps involved in the overall rate process, the activation energy for the process studied was calculated from the relationship:

$$J = A \exp(-H/kT)$$

where J is the rate of the process; A, a constant; k, the Boltzmann constant; T, the absolute temperature; and H the activation energy term encompassing all the steps. Rindone explains that the value for the complex activation energy term H can be determined either by plotting log crystallization rate versus $1/T$ and measuring the slope, or by a calculation employing:

$$H = \frac{\ln J_1 - \ln J_2}{1/T_2 - 1/T_1}$$

Using this equation the activation energy for crystallization of lithium disilicate from lithium silicate glass is calculated as 120 kcal/mole without platinum, 50 kcal/mole at 0.005 weight percent platinum, and 60 kcal/mole for further platinum additions.

Jaccodine⁽²⁰⁾ also studied the crystallization of lithium disilicate from a lithium silicate glass containing 30 mole percent Li_2O . Determining growth rates

at three temperatures, 520, 560, and 600°C and plotting log rate versus reciprocal absolute temperature, an activation energy of 49 kcal/mole was determined for crystallization of this material.

Bergeron and Russell⁽²¹⁾ studied the temperature dependence of growth rates for lead titanate, PbTiO_3 , from a $\text{PbO-B}_2\text{O}_3\text{-TiO}_2$ glass. Growth rates in microns/minute were determined from the slope of crystal size versus time plots at several temperatures. The log of these growth rates plotted against $1/T$ indicates the activation energy for growth in the temperature range 600 to 750°C is 34 kcal/mole. The activation energy for viscous flow in the same temperature region is 75 kcal/mole.

Chen,⁽¹⁸⁾ in his investigation of crystallization kinetics of a synthetic mica glass, reports an activation energy for growth of the intermediate phase described previously as 84 kcal/mole. Using an analytical technique similar to that of Bergeron and Russell described above, obtaining growth rate values at 630, 750, 800, and 830°C, Chen plotted the slopes of these curves against reciprocal absolute temperature to obtain the reported activation energy.

Some attempts to develop empirical equations for growth rate are reported in the literature. Preston⁽²²⁾ suggested an equation of the form:

$$\dot{g} = \frac{K\Delta T}{\eta}$$

which was subsequently modified by Swift⁽²³⁾ as:

$$\dot{g} = \frac{K\Delta T}{\eta^n}$$

where \dot{g} is the rate of crystal growth, K is a constant, ΔT is the undercooling in degrees, η is the coefficient of viscosity in poises, and n, a constant.

While these equations do not describe growth rates sufficiently in all glass crystallization investigations, the influence of viscosity and degree of undercooling is strikingly evident. It should be noted that more complex relationships have been developed, such as by Brown and Ginell⁽²⁴⁾ of the form:

$$\dot{g} = \frac{m_1 T e^{-W_1/T} [1 - e^{-\gamma(T_L/T - 1)}]}{1 + m_2 e^{-W_2/T}}$$

where \dot{g} is growth rate in microns/minute; T, absolute temperature; T_L , liquidus temperature; m_1 , m_2 , W_1 , W_2 , and γ , empirical constants. However, the physical meaning of these five constants was not defined.

2. Volume Transformation

Freiman and Hench⁽²⁷⁾ report the use of the JMA (Johnson-Mehl-Airami) equation for describing the kinetics

of processes where nucleation and growth occur together. An equation to describe the volume fraction of new phase, V_v of the form:

$$V_v = 1 - \exp - \left[\int_{t'=0}^{t'=1} g I G^n (t-t')^n dt' \right]$$

is employed,

where

g = a form factor

G = $G_x G_y G_z$, the growth rate

I = nucleation rate

t' = time at which a given particle nucleated

n = an integer which depends on the dimensionality of the growth mechanism. ($n = 2$ for two dimensional growth).

Assuming both the growth rate G and nucleation rate I to be independent of time, the time necessary to attain a given volume fraction of new phase, $t_{(V_v)}$ at any temperature T is defined by the relationship:

$$\ln t_{(V_v)} = \frac{Q_I + nQ_G}{(n+1)R} \cdot \frac{1}{T} + \frac{\ln G_o^n I_o g / \ln \left(\frac{1}{1-V_v} \right)}{n+1}$$

where Q_I and Q_C are the activation energies for nucleation and crystal growth respectively. A plot of logarithm time to form a given V_v against reciprocal absolute temperature yields a slope equal to:

$$\frac{Q_I + nQ_C}{(n+1)R}$$

Using this technique the authors report combined activation energy terms for crystallization of $Li_2Si_2O_5$ from glasses in the $Li_2O \cdot SiO_2$ system in the range from 49 to 92 kcal/mole.

III. EXPERIMENTAL PROCEDURE

A. Sample Preparation

1. Raw Materials

The molecular and batch compositions of the mica glass are shown in Table I along with raw material sources. The raw materials, all -200 mesh, were calcined at 200°C for 24 hours and stored in a desiccator prior to batching. Batches were weighed on a two pan balance and mixed in a twin shell blender with intensifying bar for one hour. The raw batch was stored in tightly sealed glass jars prior to melting.

2. Melting and Forming

Two major problems were encountered in attempts to fabricate the mica glass samples: evolution of fluorine or fluorine compounds during melting, and crystallization of the melt upon cooling. Several melting techniques were evaluated. Initially flat envelopes, one inch square, fabricated from .0015" platinum foil and capable of containing approximately one gram of raw batch were employed. Although melting appeared complete after 30 minutes at 1250°C in these containers, crystallization was apparent, even though the samples were water quenched. In addition weight loss measurements indicated an excessive loss of fluorine, and therefore this approach was abandoned.

A second melting technique using pressed pellets of raw batch contained in lucalox rings faced with platinum

TABLE I
Batch Compositions for $K_2Mg_5Si_8O_{20}F_4$ Glass

A. Stoichiometric Batch

<u>Raw Material</u>	<u>Number of Moles</u>	<u>Batch Weight (Grams)</u>	<u>Weight Percent</u>
K_2SiF_6	2/3	149.3	17.84
MgO	5	201.5	24.05
SiO_2	7 1/3	440.0	52.50
K_2CO_3	1/3	46.1	5.51
			100.00

B. 50 Mol Percent Excess Fluorine

<u>Raw Materials</u>	<u>Number of Moles</u>	<u>Batch Weight (Grams)</u>	<u>Weight Percent</u>
K_2SiF_6	1	220.4	26.16
MgO	5	201.5	23.91
SiO_2	7	420.7	49.93
		842.6	100.00

Source of Raw Materials:

SiO_2 - - Reagent Grade Silica; Fisher Scientific Company
MgO - - Ground, Fused; General Electric Company
 K_2CO_3 - Reagent Grade; Fisher Scientific Company
 K_2SiF_6 - U.S. Phosphoric Products Division, Tennessee Corporation

foil was evaluated. This entire unit was loaded with a piece of refractory brick, preheated rapidly to 1000°C and transferred to a second furnace at 1300°C. After an appropriate soaking time at 1300°C, usually 30 to 45 minutes, the samples were quickly extracted from the furnace and quenched using compressed air. Although weight loss data indicated a significantly higher fluorine retention than in the previous technique, devitrification of samples upon quenching was still encountered.

Considering the nature of this study it was apparent that a large number of samples with identical thermal history was mandatory. Therefore an entirely different melting technique was attempted at this point. A silica fireclay crucible with a 1/16" diameter bottom hole and tightly fitting lid was employed as the batch container. A metallurgical scorifying dish was found to form a tight seal when pressed inside the silica crucible. The capacity of this container was about 150 grams of batch. The batch material used in this technique was that given in Table I with a 50 mole percent excess of fluorine. Additions of ground glass cullet from previous melts were made to enhance melting. The charge was placed in the container and loaded into a specially designed electric resistance (glo-bar) furnace, containing a bottom hole approximately 1 inch in diameter. The crucible was carefully centered over the furnace opening, the furnace heated to 1300°C over a two hour period, held at that temperature for one

hour, and quickly raised to 1400°C. After a short period of time at 1400°C the glass commenced to flow through the crucible orifice, falling onto a 1/2" thick stainless steel plate positioned below the furnace. As the droplets of molten glass struck the plate, they were immediately quenched by manual pressing with a second metal plate. Using this technique a large number of samples in the form of discs approximately 1/16" thick and 1/2" diameter were obtained from a single melt.

3. Sample Selection

An extremely careful selection procedure was employed to further reduce any gross differences which might exist among these samples. Any samples exhibiting bubbles, raw batch, or localized opacity were discarded. The density of all samples remaining was measured and only those of density $2.525 \pm .005 \text{ gm/cm}^{-3}$ were selected for further analysis. This was the lowest density range of any samples formed and this group was selected for its high fluorine content, as will be discussed later.

4. Sample Treatment

Two ranges of heat treatment were chosen for analysis. One group of samples was treated at temperatures of 560°, 580°, 600°, and 625°C, covering the range of intermediate phase development. A second group was treated at temperatures of 1070°, 1100°, 1125°, and 1150°C where previous reports indicated that the fluormica crystals commenced to grow at significant rates. Samples were

placed in the furnace at the selected temperature, held for the desired time, removed and allowed to cool in air.

B. Differential Thermal Analysis

Samples of both heat-treated and as-quenched glasses were ground to -200 mesh particle size in preparation for differential thermal analysis (DTA). All DTA results reported herein were obtained on an R. L. Stone thermal analysis system equipped with a micro sample holder. Ground samples were carefully weighed on an analytical balance and analyzed against an Al_2O_3 reference standard. Close thermal balance between sample and reference was maintained to minimize any drift in the thermograms. The differential analysis was conducted at a nominal dynamic heating rate of about 10°C per minute, although other rates were employed in some instances. The differential temperature was plotted on a strip chart at a ΔT sensitivity of approximately 0.02 mV per inch.

C. Density Measurements

All density determinations were made on an AGR densitometer using the settling method as described by Knight.⁽²⁵⁾ In this technique samples are placed in a glass test tube containing a mixture of two heavy liquids, α -bromonaphthalene (density 1.482 gm/cm^{-3}) and s-tetra-bromoethane (density 2.96 gm/cm^{-3}). The liquids are mixed in proper ratios to produce a solution of density slightly greater than both the samples and a standard glass sample

of known density. The entire tube is contained in a water bath which is heated at a constant rate. Temperatures are recorded at which the samples and standard pass a reference line on the tube as the liquid density decreases with heating. The sample densities are calculated from predetermined coefficients for density change of the liquid with temperature. The specific formula employed in this calculation, as given by Knight⁽²⁵⁾ is:

$$D_x = D_s + F(T_x - T_s)$$

where

D_x \equiv the density of the sample
or unknown

D_s \equiv density of the standard

F \equiv temperature density factor for
the liquid; in this case
(- .0017 gm/cm³/°C)

T_s \equiv reference temperature for
the standard

T_x \equiv reference temperature for
the unknown

D. X-ray Diffraction

Thermally treated specimens were analyzed by X-ray diffraction using the Debye-Scherrer camera technique. Samples were prepared by grinding until all the powder passed through a 200 mesh screen. Diffraction patterns were obtained on a Norelco X-ray unit using CuK_α radiation

and a Ni filter. Camera exposures were for three hours.

E. Microscopic Examination

Microscopic examination of samples was conducted both on a Cambridge Scanning Electron Microscope and a JEM 7 100kv conventional electron microscope. The scanning electron microscope permits direct examination of samples with a minimal amount of preparation. The samples investigated herein were etched for one minute in 5% HF solution and coated with a conductive layer of chromium.

Replicas for examination in the electron microscope were platinum preshadowed carbon. Both etched and unetched fracture surfaces were examined. For the etched specimen, a fresh fracture surface was immersed in 1% HF solution for several seconds then rinsed in water, methanol, and dried in warm flowing air. Platinum shadowing at an angle of about 25° was evaporated on the fracture surface followed by carbon evaporation from directly above. The replicas were removed from the specimen by floating off in distilled water. On some occasions a drop of very dilute HF solution was necessary to facilitate removal of the replica.

IV. EXPERIMENTAL RESULTS

A. Chemical Analysis

Two series of chemical analyses were performed on glasses during the course of this study. A group of six samples representing combinations of various batches and melting techniques employed early in the investigation were analyzed for fluorine content only. A separate analysis was performed on the final melt D-6 which was employed in the density, electron microscopy and X-ray determinations reported below. These analyses were performed at the U.S. Bureau of Mines in College Park, Maryland and Spectrochemical Laboratories, Incorporated in Pittsburgh, Pennsylvania, respectively. The fluorine analysis performed at the U.S. Bureau of Mines was by wet techniques while the analysis from Spectrochemical Laboratories was by X-ray fluorescence. The results of these analyses are shown in Table II.

B. Differential Thermal Analysis

A typical thermogram obtained from the quenched glass is shown in Figure 2. The two most distinctive features are the slight endotherm in the 550°C region followed by a sharp exotherm between 600 and 700°C.

One parameter having a profound influence on the exothermic peak position is the fluorine content of the glass. This became apparent early in the investigation

TABLE II
Chemical Analyses of Glass Samples

Analysis Number 1 - U.S. Bureau of Mines, College Park,
Maryland

<u>Sample Number</u>	<u>F⁻, Weight Percent*</u>
N2	8.85
N3	10.30
N8	10.30
N4A	9.89
MS1C	8.86
S1F	8.73

Theoretical Fluorine Content, wt. % for $K_2Mg_5Si_8O_{20}F_4$ is
9.26%

Analysis Number 2 - Spectrochemical Laboratories, Inc.,
Pittsburgh, Pennsylvania

<u>Component</u>	<u>Theoretical Weight Percent</u>	<u>Melt D-6</u>
K ₂ O	11.48	9.30
MgO	24.57	25.70
SiO ₂	58.59	52.70
F ₂	9.26	10.80*
O(=F)	-3.90	----
	<hr/> 100.00	<hr/> 98.50

*Fluorine analyses ± 0.50 weight percent.

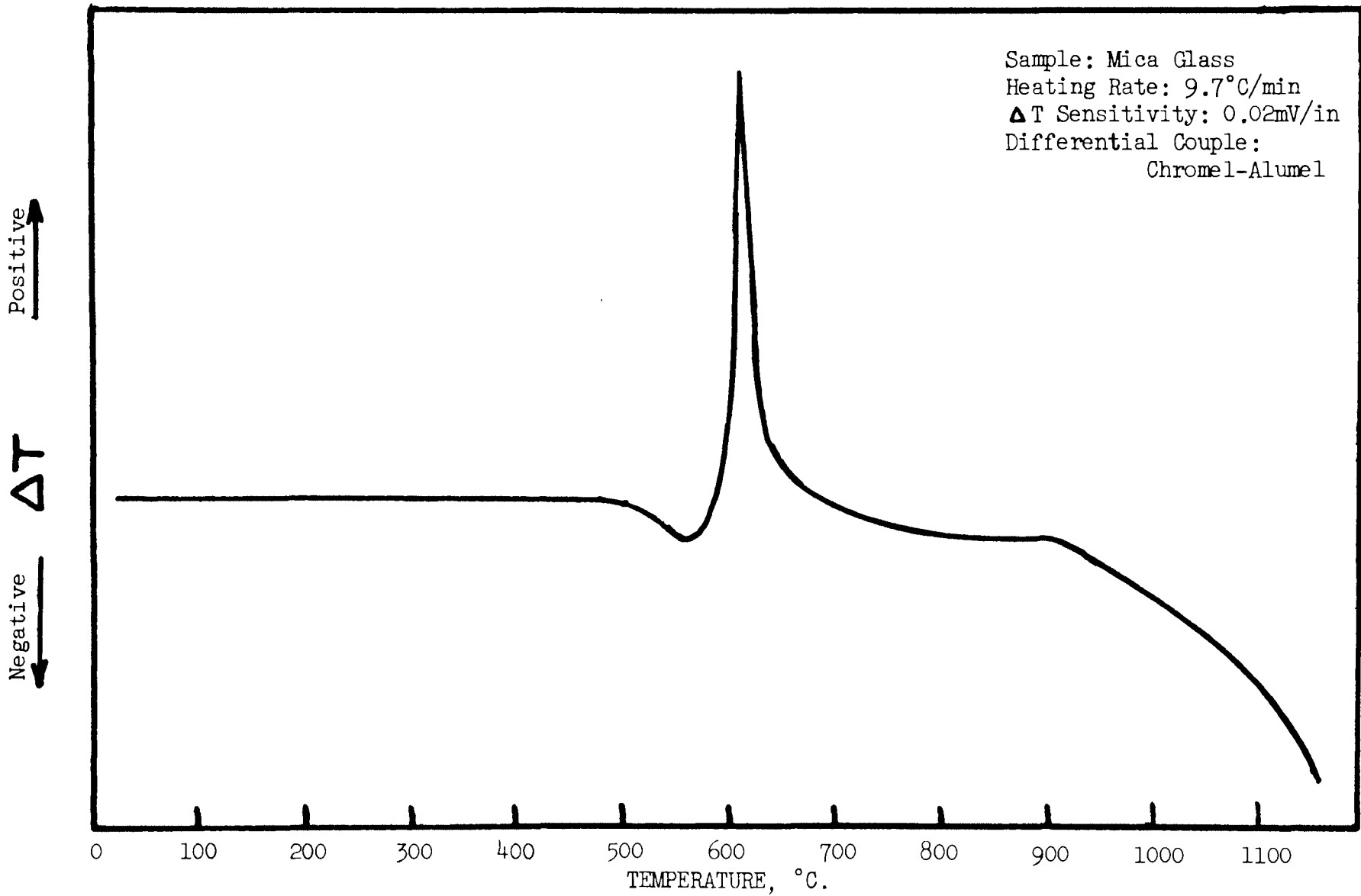


Figure 2. Typical Differential Thermal Analysis Curve For As-quenched $K_{2.5}Mg_5Si_8O_{20}F_4$ Glass

when identical experimental conditions - sample weight, reference weight, particle size, and heating rate - resulted in varied exothermic peak temperatures for samples from different melts. Later chemical analyses revealed that these samples contained quite varied amount of fluorine. Table IV shows this trend for a series of samples with different fluorine contents.

A series of thermograms was also run on glass samples of varying particle size from a single melt. Size ranges, through 48 on 100, 100 on 200, and 200 on 325 mesh, all from a single piece weighing 10 mg., were analyzed. Essentially no variation in exothermic peak intensity or temperature was observed among this group of samples.

A series of DTA thermograms was also obtained on a group of isothermally treated specimens. Figure 3 shows the results of treating the glass at 600°C for periods of 1/2, 1, 2, 3, and 4 hours. After four hours only a very slight indication of exothermic behavior is evident. Similar treatments at 620 and 640°C as shown in Figure 4 reveal the same behavior trend proceeding much more rapidly. At 620°C for two hours and 640°C for thirty minutes the exothermic peak had essentially disappeared for the thermograms.

C. Density Measurements

As earlier noted, the lowest exothermic peak temperature was associated with the highest fluorine content.

TABLE III
Variation of Exothermic Peak
Temperature with Fluorine Content

<u>Sample</u>	<u>Fluorine Content (Weight Percent)</u>	<u>Exothermic Peak Temperature (°C)*</u>
S1F	8.73	658
N2	8.85	650
MS1C	8.86	652
N4A	9.89	648
N3	10.30	639
N8	10.30	636
D6	10.80	608

*Accuracy of reported peak temperatures $\pm 5^{\circ}\text{C}$.

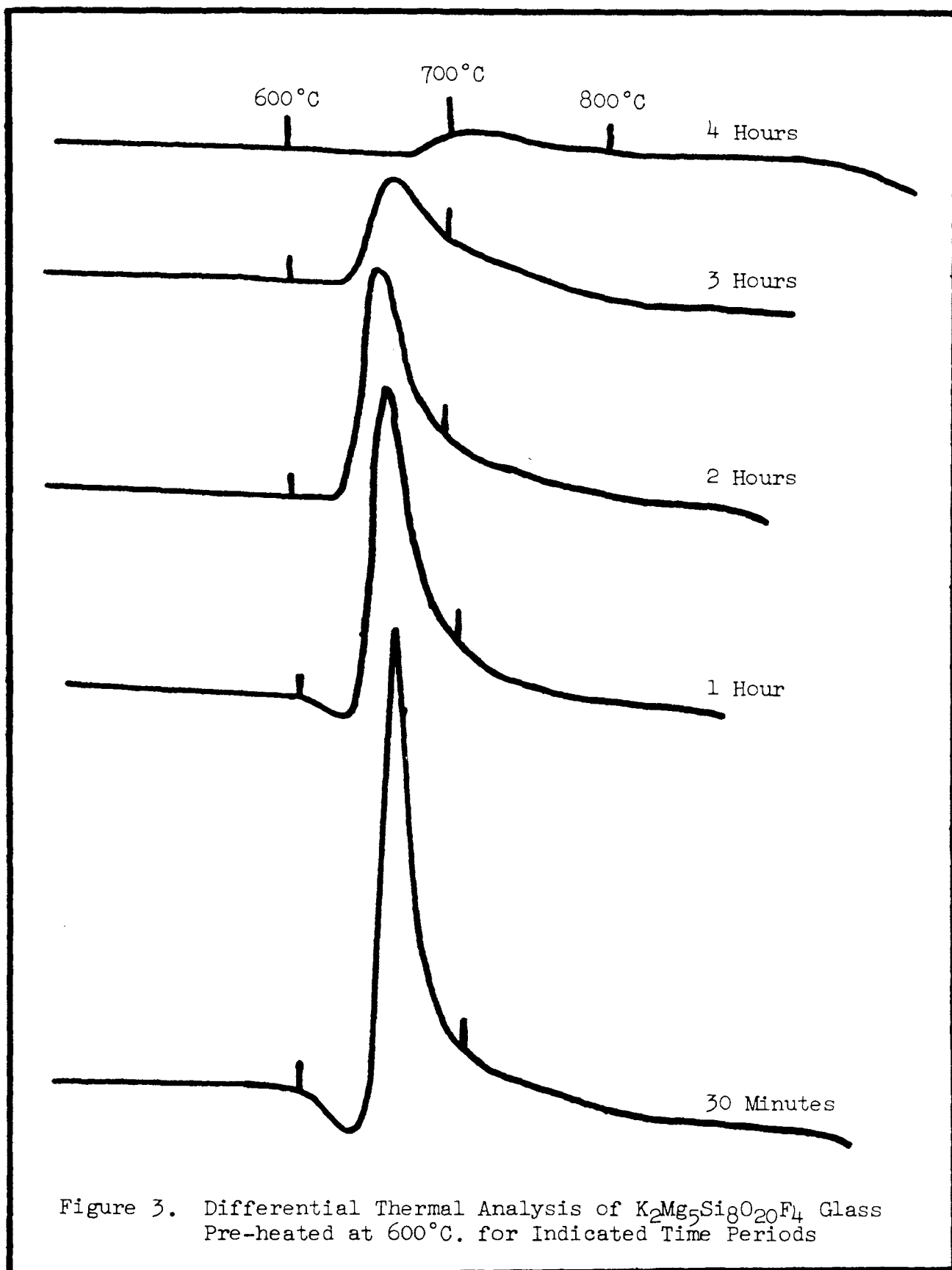


Figure 3. Differential Thermal Analysis of $K_2Mg_5Si_8O_{20}F_4$ Glass Pre-heated at $600^\circ C$. for Indicated Time Periods

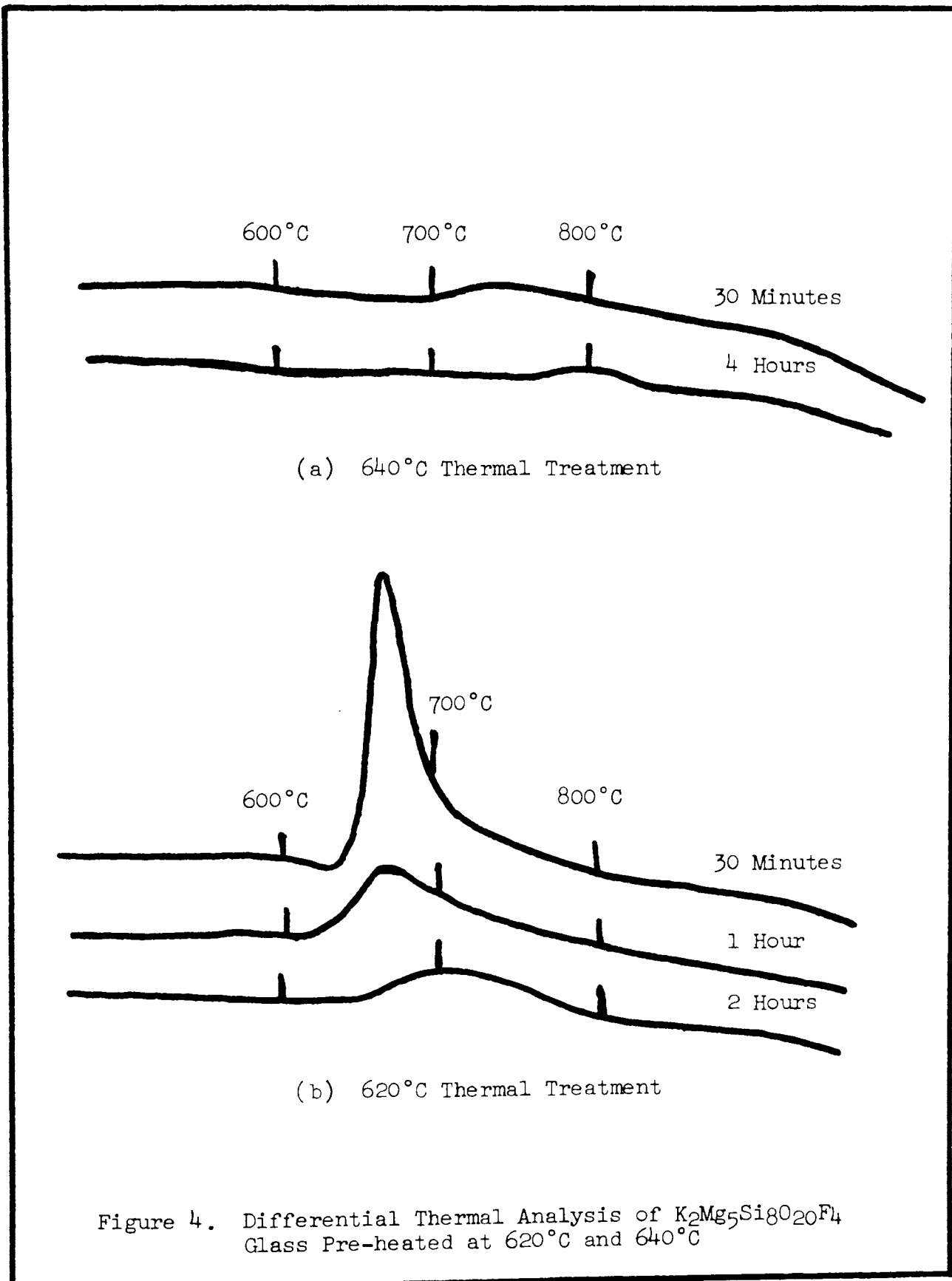


Figure 4. Differential Thermal Analysis of $K_2Mg_5Si_8O_{20}F_4$ Glass Pre-heated at $620^\circ C$ and $640^\circ C$

Since the lowest peak temperature and sharpest peaks were exhibited by samples of the lowest density, all samples subsequently employed for density, X-ray diffraction, and microscopic analysis were of a similar low density ($2.525 \pm .005 \text{ gm/cm}^3$).

Figure 5 shows the density behavior of glass samples heated at 560, 580, 600, and 625°C as a function of time. The tendency to plateau after short periods of time is strong, above 580°C.

Figure 6 shows the density changes with time for samples heated at 1070, 1100, 1125, and 1150°C. For the 1100 and 1125°C isotherms, the density approaches that of the crystalline mica. However at 1150°C, the material exhibits a maximum density followed by a dramatic decrease in density with extended treatments.

D. X-Ray Diffraction

Powder X-ray camera patterns of glass specimens heat treated for various times at temperatures from 560 to 625°C are shown in Figures 7 through 9. The first evidence of significant structural change is seen in Figure 7 for the specimen treated for nine hours at 560°C. In Figure 8 the faint lines in the 580°C - 30 minute specimen treatment indicate that structural ordering has commenced. Increased treatment times at this same 580°C temperature produce only slight variation of intensity of these lines as seen in the remaining patterns in Figure 8. The diffraction patterns

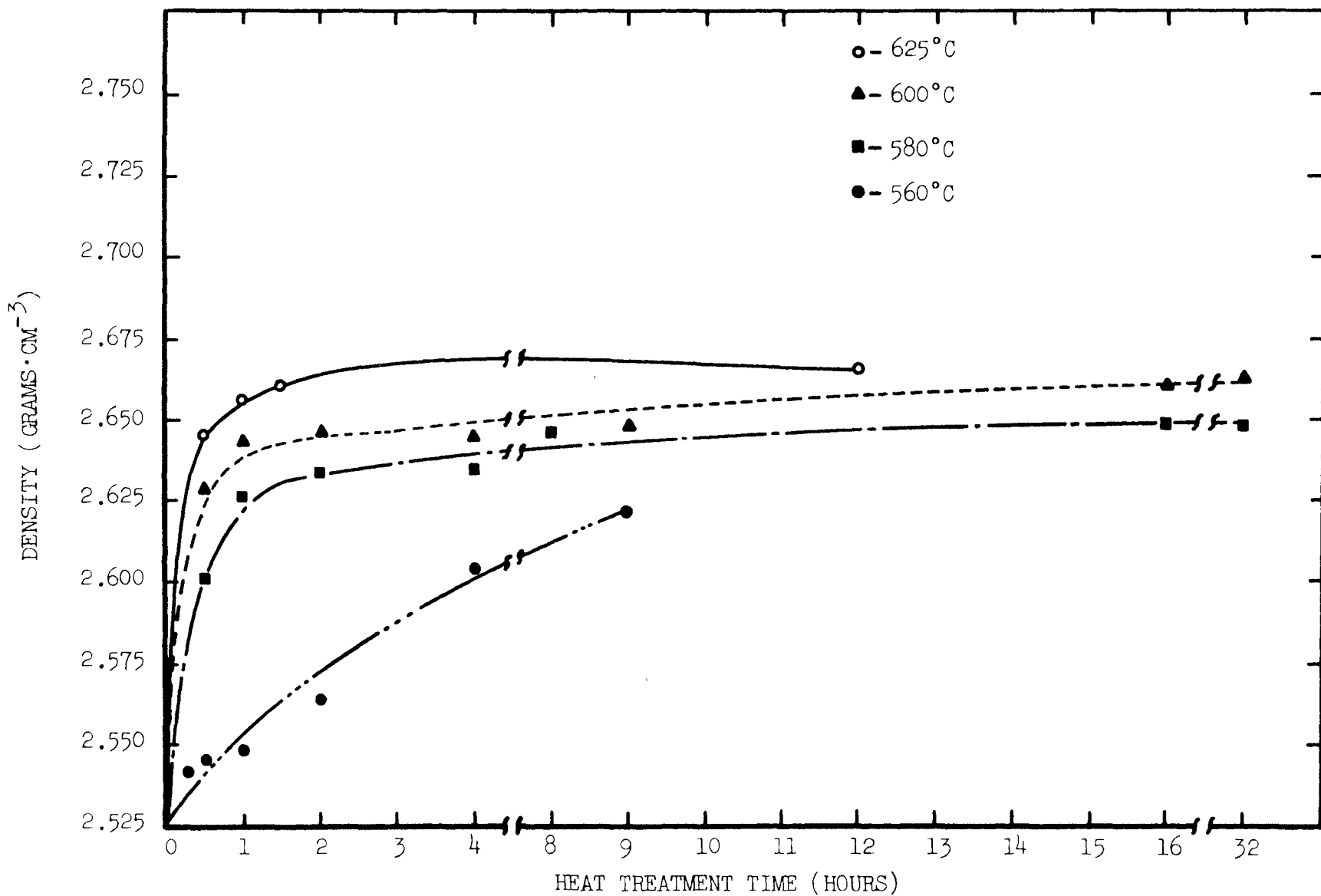


Figure 5. Density vs. Heat Treatment Time at 560° to 625°C for $K_2Mg_5Si_8O_{20}F_4$ Glass

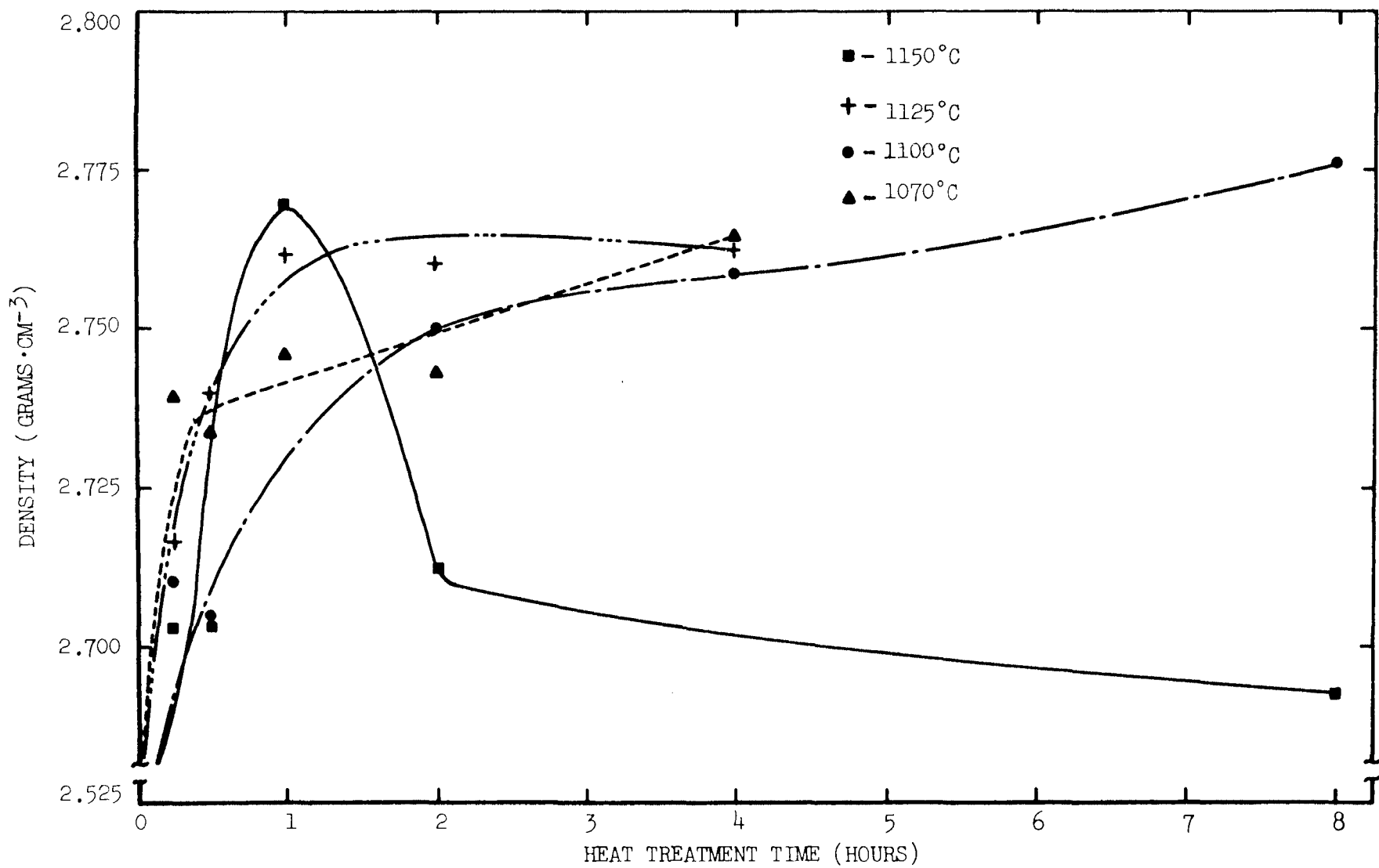


Figure 6. Density vs Heat Treatment Time at 1070° to 1150°C for $K_2Mg_5Si_8O_{20}F_4$ Glass

(a) Glass as
quenched.



(b) 15 minutes
at 560°C.



(c) 30 minutes
at 560°C.



(d) 1 hour
at 560°C.

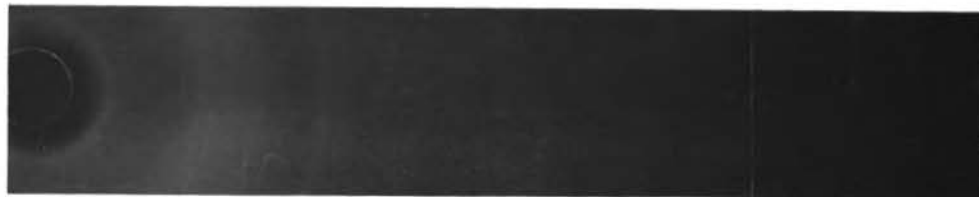


(e) 9 hours
at 560°C.



Figure 7. X-ray Diffraction Patterns of $K_2Mg_5Si_8O_{20}F_4$ Glass
- as quenched and Treated Isothermally at 560°C.

(a) 30 minutes
at 580°C.



(b) 1 hour
at 580°C.



(c) 2 hours at
580°C.



(d) 4 hours
at 580°C.



(e) 8 hours
at 580°C.



(f) 32 hours
at 580°C.



Figure 8. X-ray Diffraction Patterns of $K_2Mg_5Si_8O_{20}F_4$ Glass Heat Treated Isothermally at 580°C.

(a) 30 minutes
at 600°C.



(b) 16 hours
at 600°C.



(c) 30 minutes
at 625°C.



(d) 4 hours
at 625°C.



Figure 9: X-ray Diffraction Patterns of $K_2Mg_5Si_8O_{20}F_4$ Glass Heat Treated Isothermally at 600° and 625°C.

shown in Figure 9 for treatments at 600 and 625°C appear essentially unchanged from the pattern for a specimen held at 580°C for 32 hours.

The diffraction patterns from samples heated at temperatures from 700 through 1000°C show lines of increased sharpness and intensity. A representative series of these patterns is shown in Figure 10. Patterns of samples heated at 1070 to 1150°C for short time periods along with the pattern for a $K_2Mg_5Si_8O_{20}F_4$ standard sample are presented in Figure 11. The tetrasilicic fluormica material used as a standard was produced by melt crystallization at the U. S. Bureau of Mines, Norris, Tennessee Electrotechnical Research Laboratory (This facility is no longer in operation.). The patterns obtained from samples treated at 1070°C show mica to be the only phase and identical to the standard material. (Intensities are weaker partly because of coarser particle size of the heat treated materials.)

E. Electron Microscopy

The majority of the electron microscopy work reported herein was performed on samples heat treated from 560 to 625°C. Some survey work was done on a few specimens treated at temperatures between 625 and 1000°C. Typical microscope findings are shown in Figures 12 and 13. Etching procedures never resulted in electron micrographs exhibiting consistent microstructure within a given temperature group; consistently good pictures were obtained from unetched



(a) 16 hours
700°C.



b) 64 hours
at 800°C.



(c) 32 hours
at 900°C.



(d) 8 hours
at 1000°C.

Figure 10. X-ray Diffraction Patterns of $K_2Mg_5Si_8O_{20}F_4$ Glass Heat Treated at 700°C, 800°C, 900°C, and 1000°C



(a) Tetrasilicic
Mica Standard.



(b) 30 minutes at
1100°C.



(c) 30 minutes at
1125°C.



(d) 30 minutes at
1150°C.

Figure 11. X-ray Diffraction Patterns of $K_2Mg_5Si_8O_{20}F_4$ Glass Heat Treated at 1100°C, 1125°C, 1150°C and $K_2Mg_5Si_8O_{20}F_4$ Standard Pattern

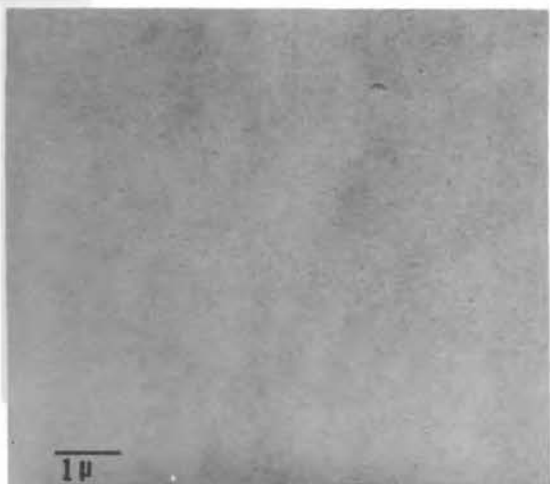
fracture surfaces. All electron micrographs shown herein are from replicas of unetched fracture surfaces.

Figure 12a shows the unetched fracture surface of the glass as quenched. Subsequent heat treatment at 560°C for times of 15 minutes through 9 hours produced little apparent ordering as shown in Figure 12b through 12f. No distinct phase appearance can be discerned in these micrographs. Replicas examined from the 580°C heat treatment series exhibited this same type of microstructure.

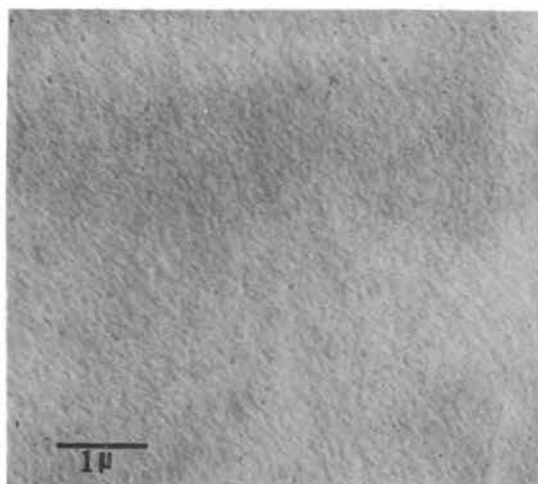
The microstructures of samples treated at 600°C for 32 hours, 800°C for 64 hours, and 900°C for 32 hours are shown in Figure 13a through c, respectively. Treatment at 600°C for 32 hours reveals no indication of distinct particle development. Comparing Figures 13a and 12c, there is no evidence of increase in crystalline particle development from the 32 hour 600°C treatment over that at 560°C for 9 hours.

The first distinct indication of microstructure development is shown in Figure 13b, a replica of an unetched fracture surface treated at 800°C for 64 hours. The phase appears as rounded particles or areas with no evidence of the characteristic blocky mica habit.

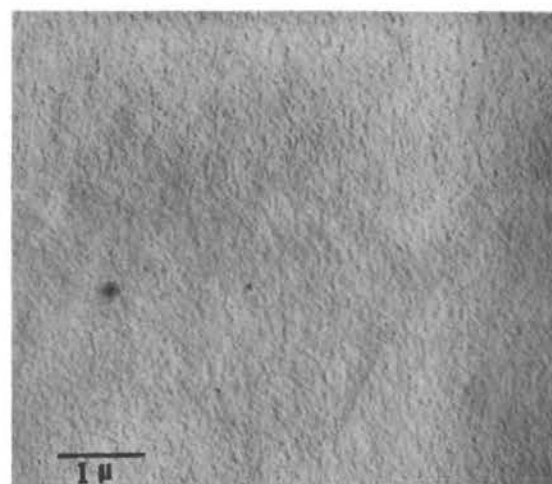
The existence of distinct mica like particles is clearly indicated in Figure 13c. This is a replica from an unetched fracture surface of a sample treated at 900°C for 32 hours. The mica particles are distributed throughout a matrix of the rounded particles evident in Figure 13b.



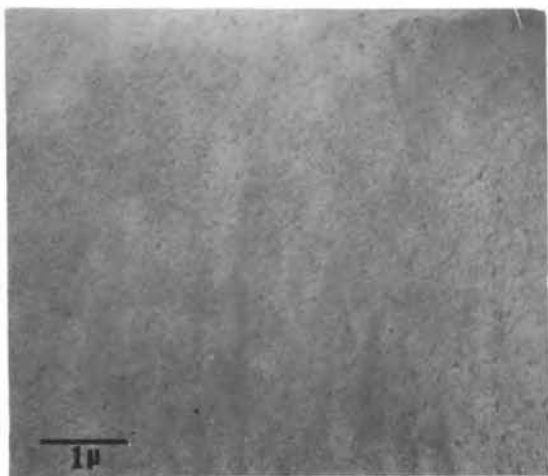
(a) Glass as quenched



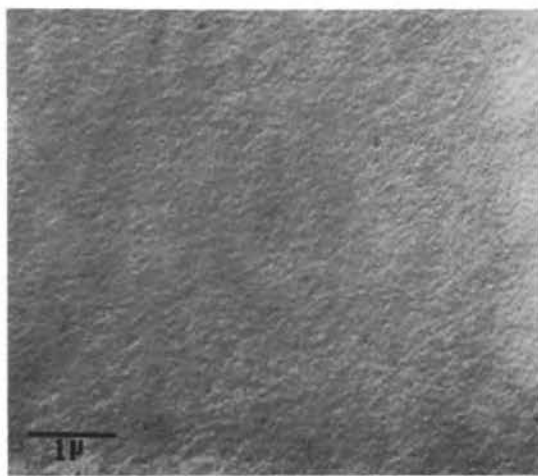
(b) 15 minutes at 560°C



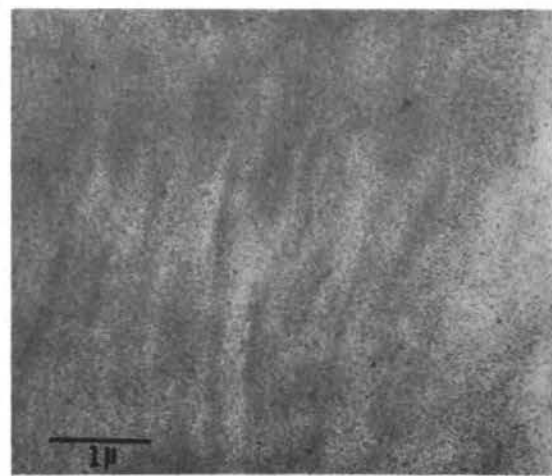
(c) 30 minutes at 560°C



(d) 1 hour at 560°C



(e) 2 hours at 560°C

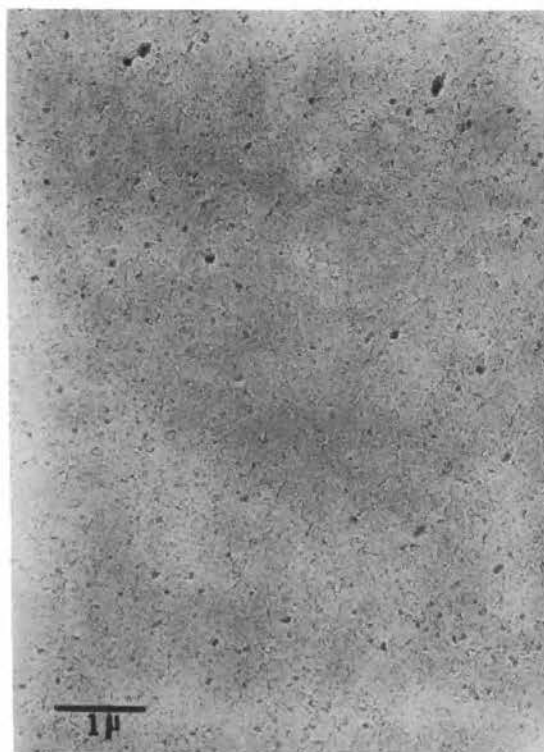


(f) 9 hours at 560°C

Figure 12. Electron Micrographs of As-quenched $K_2Mg_5Si_8O_{20}F_4$ Glass and 560°C Isothermal Heat Treatments



(a) 32 hours at 600°C.



(b) 64 hours at 800°C.



(c) 32 hours at 900°C.

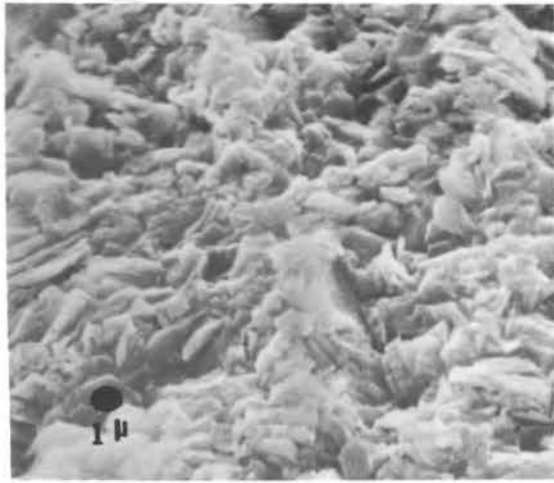
Figure 13. Electron Micrographs of $K_2Mg_5Si_8O_{20}F_4$ Glass Heat Treatments at 600°C, 800°C, and 900°C

F. Electron Scanning Microscopy

Electron scanning micrographs for a series of specimen thermally treated at 1100, 1125, and 1150°C are shown in Figures 14 through 16. Growth of particles and development of structure in the progression of increasing time at single temperatures and with increasing temperature is evident in this series of photomicrographs. The flat blocky particles characteristic of mica materials are well developed through the longer treatment times at 1125 and 1150°C.

G. Phase Transformations

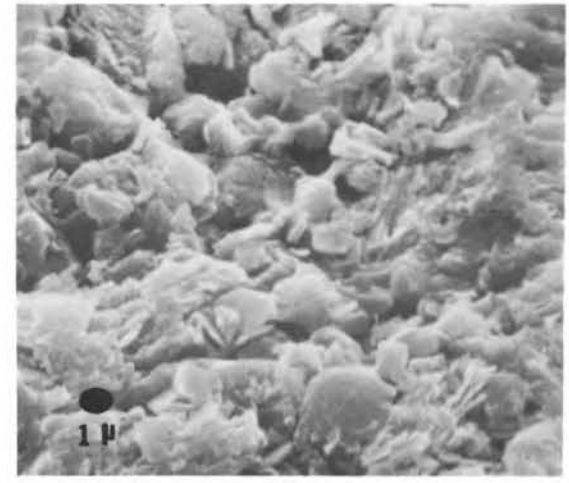
Experiments were designed to determine the kinetics of phase transformations in two temperature regions during crystallization of the mica glass. Two techniques were employed. In the 600°C region the volume transformed at three temperatures; 580, 600, and 625°C was estimated as a function of heating time from density measurements. Using the limiting value of 2.665 grams/cc obtained at 600°C after 32 hours and 625°C after 4 hours as the theoretical 100 percent low temperature transformation density, the JMA data analysis scheme as described by Freiman and Hench⁽²⁷⁾ was employed. In this procedure, the logarithm of time necessary to attain a 50 percent volume transformation is plotted against reciprocal absolute temperature. The slope of this curve yields an activation energy term for the combined nucleation and crystal growth processes.



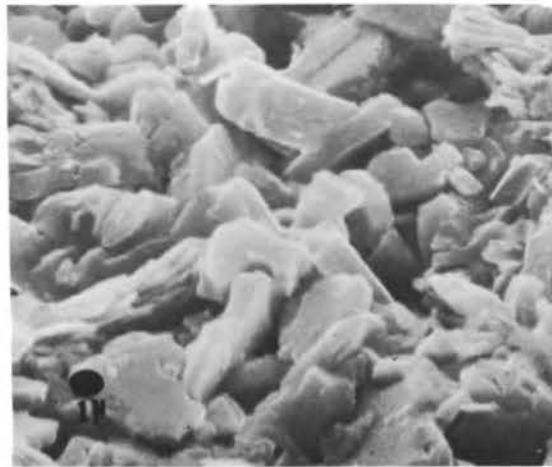
(a) 15 minutes at 1100°C.



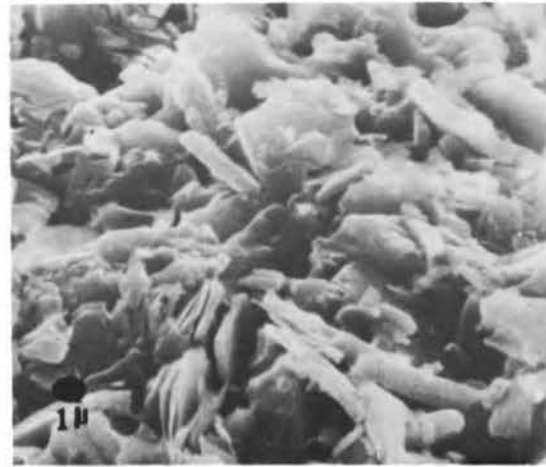
(b) 30 minutes at 1100°C.



(c) 2 hours at 1100°C.

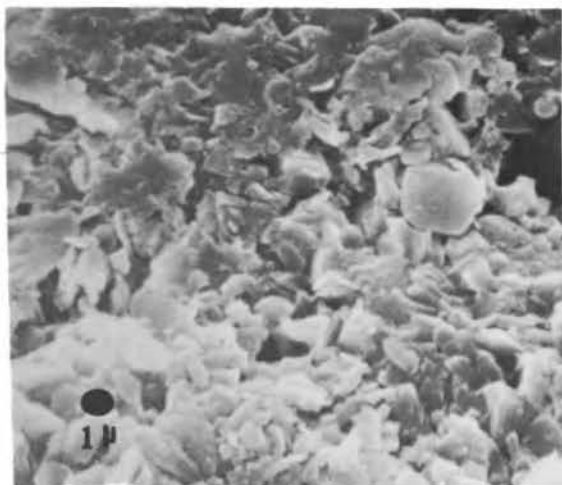


(d) 4 hours at 1100°C.

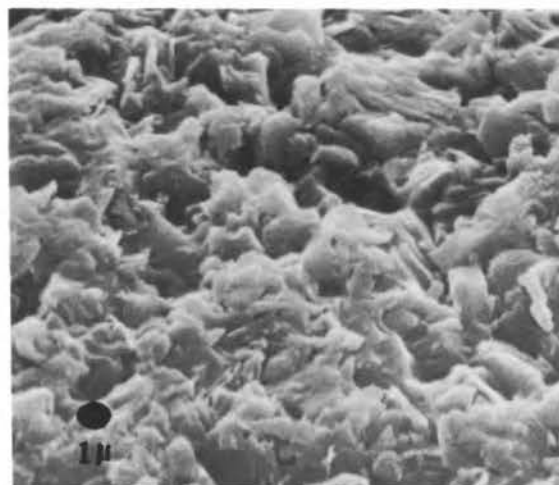


(e) 8 hours at 1100°C.

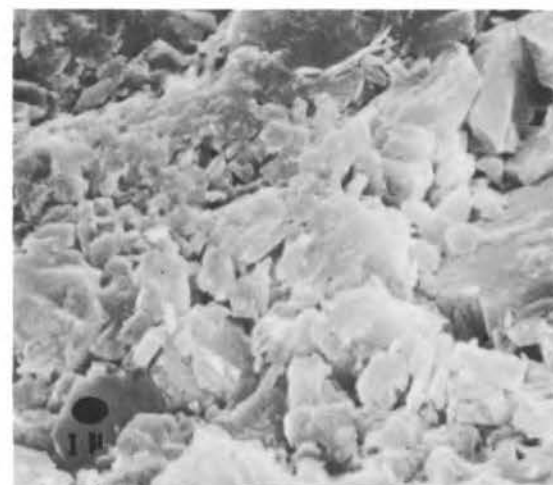
Figure 14. Electron Scanning Micrographs of $K_2Mg_5Si_8O_{20}K_4$ Glass Heat Treated Isothermally at 1100°C.



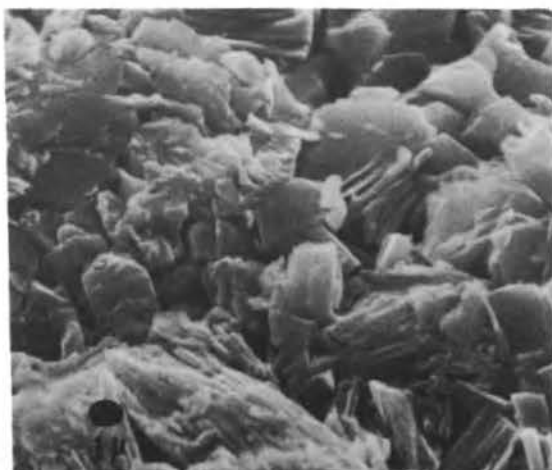
(a) 15 minutes at 1125°C.



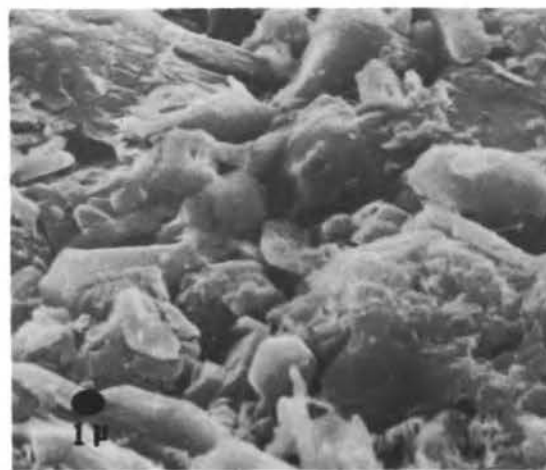
(b) 30 minutes at 1125°C.



(c) 1 hour at 1125°C.

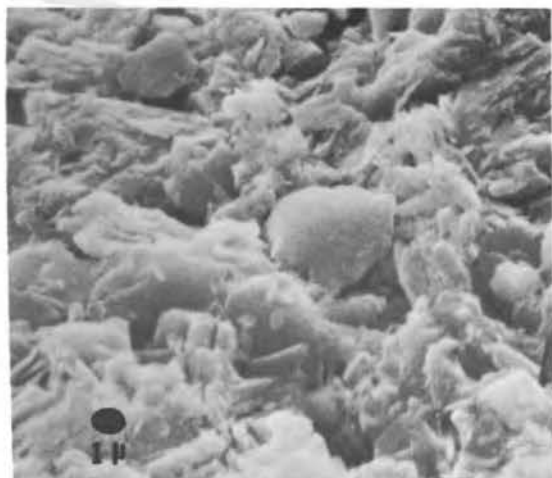


(d) 2 hours at 1125°C.

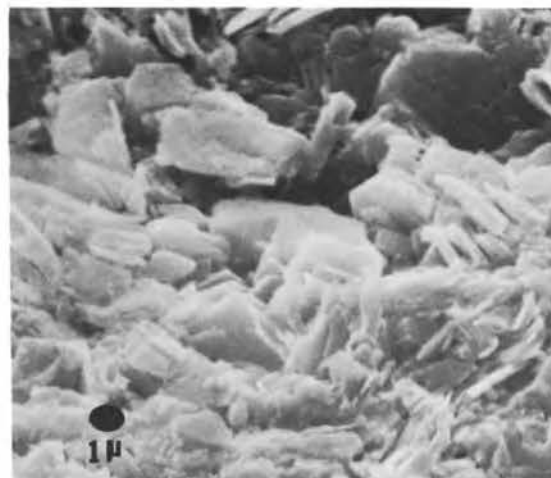


(e) 4 hours at 1125°C.

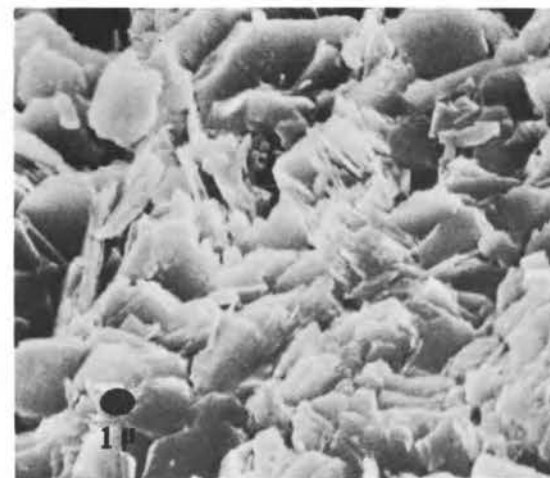
Figure 15. Electron Scanning Micrographs of $K_2Mg_5Si_8O_{20}F_4$ Glass Heat Treated Isothermally at 1125°C.



(a) 15 minutes at 1150°C.



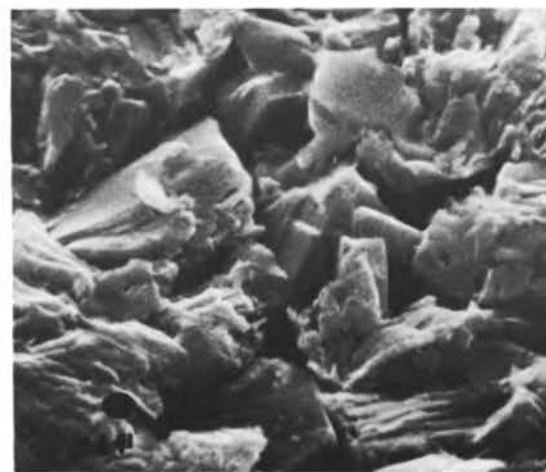
(b) 30 minutes at 1150°C.



(c) 1 hour at 1150°C.



(d) 2 hours at 1150°C.



(e) 8 hours at 1150°C.

Figure 16. Electron Scanning Micrographs of $K_2Mg_5Si_8O_{20}F_4$ Glass Heat Treated Isothermally at 1150°C.

The results of this analysis are shown in Figure 17, the curve yielding a combined activation energy value of approximately 20 kcal/mole. The technique employed in estimating the times for attainment of 50% volume transformation at 580, 600, and 625°C does not allow for rigorous error analysis. However, variation in estimation of this time could result in an uncertainty of ± 10 kcal for this low temperature activation energy value.

The high temperature transformation was studied through growth rate determinations by measuring particle size as a function of time and temperature. The largest particle at each temperature and time was measured and the results shown in Table IV. The resulting coordination plot of these data is shown in Figure 18. The slope of the initial portion of each temperature curve was calculated to obtain growth rate values at each of four temperatures. The plot of log growth rate versus reciprocal absolute temperature is shown in Figure 19. Analysis of the slope of this curve gives an activation energy for crystal growth of 30 kcal/mole. A least squares fit of these data yields a standard deviation of ± 100 kcal/mole on this determination.

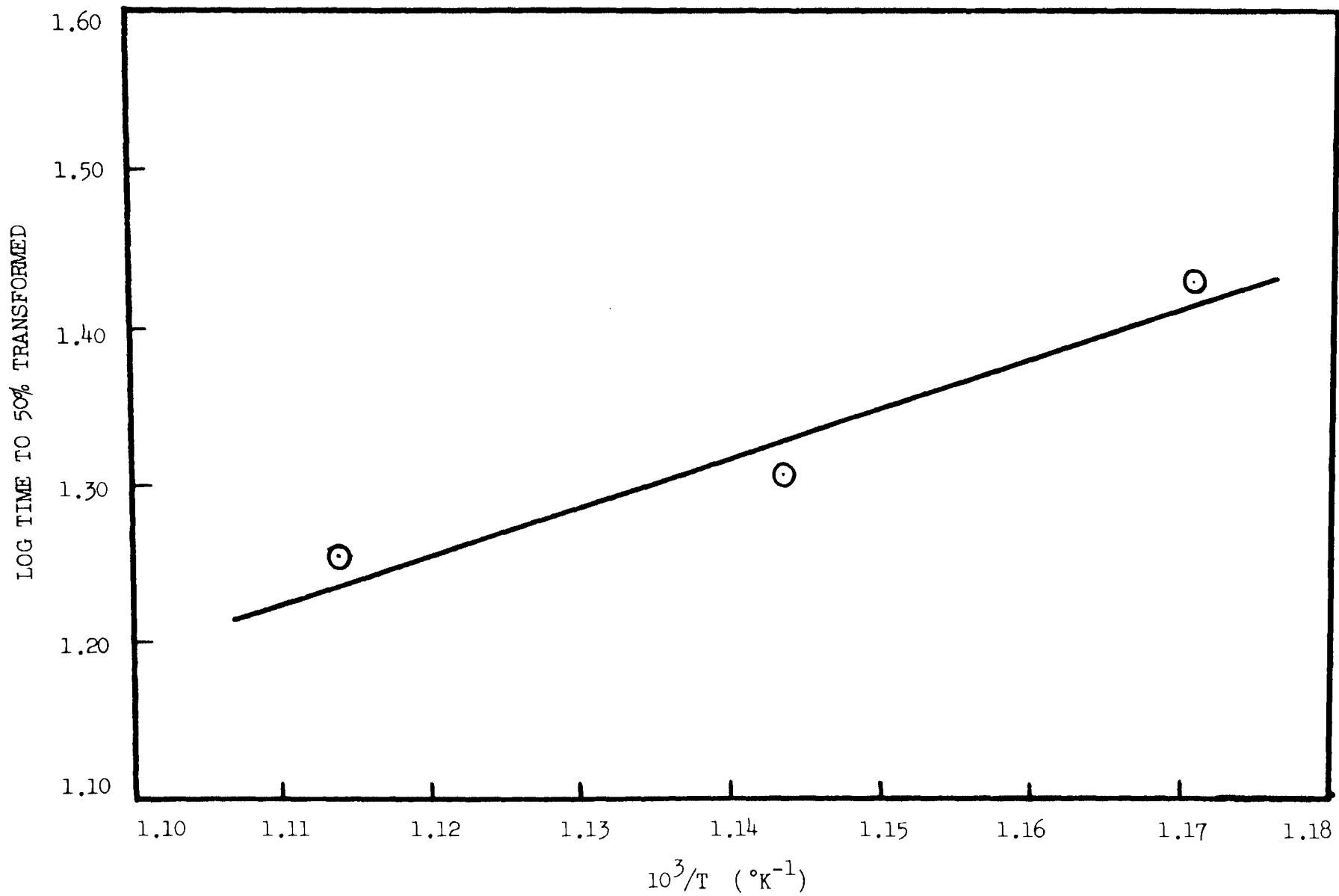


Figure 17. Temperature Dependence of Transformation Rate for $K_2Mg_5Si_8O_{20}F_4$ Glass in the 600°C Region.

TABLE IV
Results of Analysis for Largest Particle
from Electron Scanning Micrographs

<u>Temperature (°C)</u>	<u>Time (Minutes)</u>	<u>Magnification</u>	<u>Particle Size (Microns)</u>
1070	15	18,000X	0.89
1070	120	9,000X	3.06
1070	1440	1,880X	5.60
1100	15	4,760X	1.99
1100	30	4,680X	3.08
1100	120	4,430X	3.78
1100	240	4,600X	4.20
1125	15	4,600X	2.29
1125	30	4,600X	2.98
1125	60	4,510X	4.40
1125	120	4,680X	5.55
1125	240	4,760X	7.90
1150	15	4,940X	3.85
1150	30	4,680X	5.15
1150	60	4,680X	5.65
1150	120	1,975X	9.10

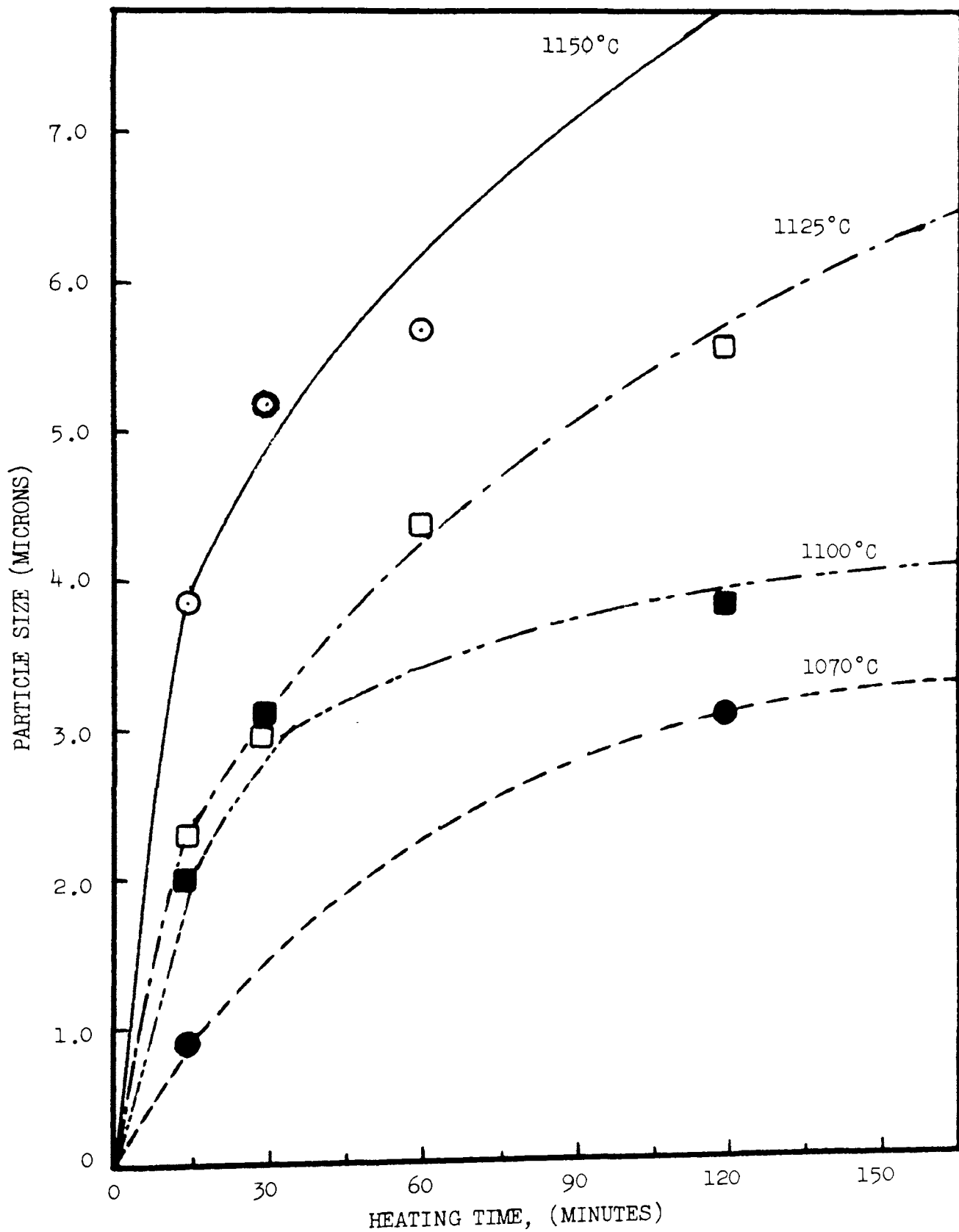


Figure 18. Particle Size of $K_2Mg_5Si_8O_{20}F_4$ Crystals Growing from Glass vs. Heating Time at Temperatures from 1070°C to 1150°C

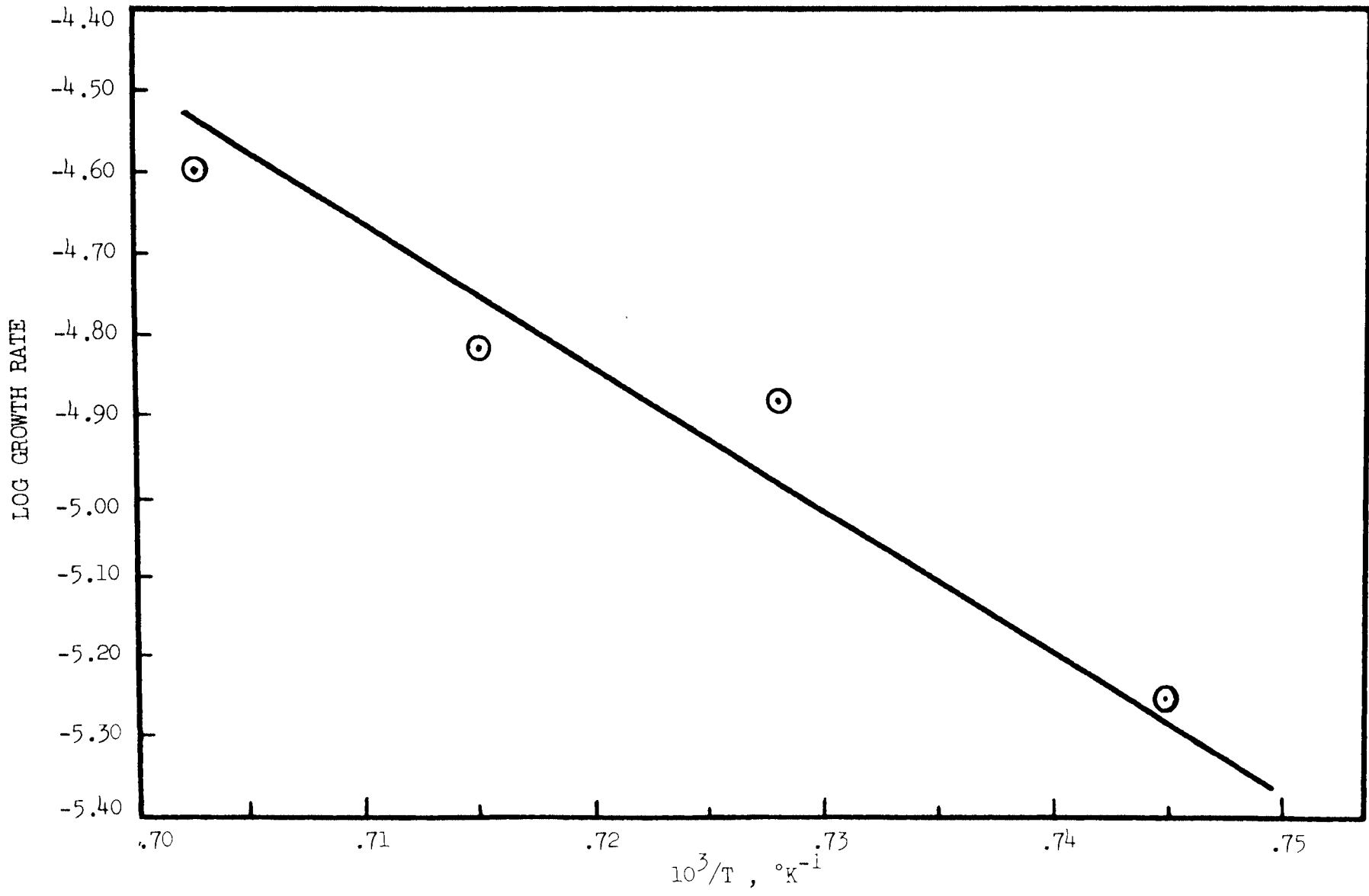


Figure 19. Crystal Growth Rate of Synthetic Mica $K_2Mg_5Si_8C_{20}F_4$ from a Glass of the Same Composition.

V. DISCUSSION OF RESULTS

A. Chemical Analysis

Loss of fluorine during melting and thermal treatment was a primary concern in this investigation. Previous investigators⁽¹⁰⁾ have shown that only the slightest deficiency in fluorine content of fluormica compounds results in decomposition to forsterite, Mg_2SiO_4 and norbergite, $Mg_3SiO_4(F,OH)_2$. Analysis of X-ray diffraction films showed no evidence of these phases being present, even for the 1150°C thermal treatment, where fluorine loss was greatest.

The chemical analysis of the final sample series does deviate from theoretical composition for $K_2Mg_5Si_8O_{20}F_4$ according to determinations performed by an independent laboratory. However, the X-ray diffraction data for the crystallized specimen from this series corresponds closely with that from the standard $K_2Mg_5Si_8O_{20}F_4$ material supplied by the U. S. Bureau of Mines. Therefore, it is not believed that the small chemical deviations have produced any secondary phases to interfere with the mica crystallization process being studied. It is important to note that the fluorine content does have an effect upon the temperature of which the transformation from amorphous to crystalline structure is initiated during heating of the quenched glass. This observation is discussed further in the following section.

B. Structural Transformations

Previous investigators^(3,4,18) report that the transformation of synthetic mica compositions from initially amorphous to crystalline structures consists of a two step process: 1) a transformation from an amorphous to an intermediate phase occurring in the 600°C region, and 2) a transformation from an intermediate to a crystalline phase above 1000°C. While this investigation was designed primarily to investigate these two transformations, intermediate temperatures were included in the thermal treatments.

1. Early Stages of the Structural Transformation

Differential thermal analysis shows a distinct exothermic peak in the 600°C region during controlled heating of the quenched glass. Subsequent differential thermal analysis of specimens treated isothermally at a number of temperatures in the 600°C temperature region show a gradual decrease in exothermic peak intensity with increasing time along any given isotherm. The decrease of exothermic peak intensity occurs more rapidly with increasing treatment temperature from 600°C to 640°C, as would be expected for thermally activated transformations. This behavior is generally associated with crystallization of an amorphous system, as described by Bergeron, et al⁽³²⁾ and Layton and Herczog.⁽³⁰⁾ Although this analysis was performed on specimens approximately 10% low in

theoretical fluorine content, the trend is significant and corresponds well with density changes observed for similarly treated specimens of fluorine content slightly above theoretical.

The series of differential thermal analyses run on specimens of various particle sizes showed no effect of this parameter on position or intensity of the exothermic peak. Tudorovskaya and Sherstyuk⁽²⁶⁾ report that glasses which nucleate and crystallize via an internal process exhibit narrow sharp exothermic peaks in differential thermal analysis, while surface processes are characterized by broad flat exothermic peaks. This information coupled with the observation that particle size has no effect on the peak position and intensity indicates that the initial transformation in the $K_2Mg_5Si_8O_{20}F_4$ glass occurs by an internal process.

Density measurements of specimens treated isothermally at selected temperatures in the 600°C region show that the transformation process approaches a limiting terminal rate after fairly short times at any given temperature. As the temperature increases the time necessary to attain this limiting density value diminishes quite rapidly. X-ray diffraction shows that this density increase is associated with the development of a distinct crystalline phase.

Initial appearance of this phase occurs at 560°C after a 9 hour treatment and at 580, 600, and 625°C after only 30 minutes. X-ray analysis of specimens treated at

625°C for 12 hours indicated essentially no change in line intensities or position from the diffraction lines for specimens treated at 580°C. Apparently the crystalline phase developing in this temperature region encounters a barrier to further crystal growth. Such a barrier could account for the limiting density values exhibited by these same specimens.

Electron micrographs of specimens treated in the 600°C region exhibited no indications of distinct structural development which could be correlated with the crystalline phase identified by X-ray diffraction. The first observation of distinct phase development occurred in specimens treated at 800°C for 64 hours. At this point irregularly shaped particles are clearly visible as seen in Figure 13b. Treatment at 900°C for 16 hours yields distinctly shaped mica-like particles embedded in an amorphous matrix phase. The X-ray diffraction films for these two treatments show lines which are much sharper than those of lower temperature treatments indicating a significant amount of crystal growth has occurred in the region between 625 and 800°C.

No electron microscope findings revealed any elongated particles as observed by Chen⁽¹⁸⁾ in his study of the glass-mica transformation for a synthetic phlogopite mica system. Chen included an unstated amount of boric oxide in his fluormica composition which could conceivably alter the nucleation and growth mechanism relative to that encountered in a pure system.

Since the micrographs did not reveal particles amenable to the determination of crystal growth rates for the early stages of the transformation process, an alternate technique as described by Freiman and Hench⁽²⁷⁾ was employed. This method yields a combined activation energy for nucleation and crystal growth. The value of 20 kcal/mole obtained for the system $K_2Mg_5Si_8O_{20}F_4$ is admittedly a first approximation considering that: 1) the data is calculated from a curve containing only three points and 2) no information on the actual density of the crystallizing phase is available. Chen⁽¹⁸⁾ reported an activation energy for crystal growth of 84 kcal/mole for his pseudocrystalline phase in the B_2O_3 --phlogopite fluormica system.

Comparing Chen's value of 84 kcal/mole with the rough estimate of combined nucleation and growth activation energy in the $K_2Mg_5Si_8O_{20}F_4$ system of 20 kcal/mole, suggests the latter system has a lower thermal barrier for the transformation. This could result from lower diffusion distances necessary for early stages of crystalline formation in the tetrasilicic system, as would be expected in a pure system where the glass is transforming to a crystalline phase of a similar composition.

2. Final Stages of the Transformation

Results of density measurements, X-ray diffraction, and electron scanning microscopy for specimens treated isothermally at selected temperatures from 1070

to 1150°C indicate that the transformation from amorphous to crystalline structure proceeds by a mechanism similar to that observed in the 600°C temperature region.

Specifically, the density values increase rapidly to a limiting terminal value and the X-ray diffraction patterns show the presence of a single crystalline phase.

After treatment times of only 15 minutes at each temperature the maximum density has been nearly achieved. The diffraction lines of these specimens are sharper and more intense, but occur at essentially the same positions as those observed in the early stages of the transformation.

The density decrease observed with extended times at 1150°C can be related to a decomposition of the crystalline phase resulting in the development of a pore phase. Such behavior is not uncommon in polycrystalline oxide systems at temperatures near the melting point, as is the case here ($K_2Mg_5Si_8O_xF_{4.5}$ melting point, 1176°C⁽⁹⁾). This decomposition is probably coupled with a weight loss known to involve fluorine as described by Alley and Shell.⁽⁹⁾

The electron scanning micrographs clearly show the development of flat blocky crystals characteristic of crystalline mica materials after treatment times of 4 hours at 1100°C. For shorter treatment times at each of these temperatures the particle morphology is irregular and quite comparable to that observed in electron micrographs

of specimens treated at 800°C for 64 hours as shown in Figure 13b.

The change of particle morphology in a crystallizing glass without a change in crystalline structure is mentioned in the literature. MacDowell⁽²⁸⁾ reports a change from spherical to tabular habit without any change in X-ray diffraction patterns in the crystallization of barium silicate glasses. The transformation of the tetrasilicic mica glass studied herein appears to behave in a similar manner.

Measurement of crystal growth rates realized in the high temperature heat treatments yields an activation energy for crystal growth of 30 kcal/mole. The decision to determine growth rates by measuring the largest particle at each treatment time and temperature was influenced by the specific behavior of the system under investigation. The severe quench necessary to form a glass of the tetrasilicic composition indicates that a significant overlap of crystal growth and nuclei formation temperature regions may exist. Blau⁽²⁹⁾ reports that this type of overlap does produce crystallization upon cooling in certain glass systems. Assuming such an overlap of nucleation and growth temperature regions does exist in the $K_2Mg_5Si_8O_{20}F_4$ composition then thermal treatments conducted to produce crystal growth may also create stable nuclei. These nuclei will subsequently commence to grow at any point in time up to the end of the isothermal treatment period. Thus,

any determination of average particle size would be biased by crystals forming and growing for time periods much shorter than that selected for the treatment. Selecting the largest particle present for any given thermal treatment implies that this particular nucleus was present at essentially zero time. While the statistical basis for this approach is weak, the growth rate of this one particle is believed to yield a reasonable value for evaluating the mechanism of the transformation process.

Comparing the value of 30 kcal/mole for the activation energy for crystal growth at high temperatures with the value of 20 kcal/mole for the activation energy of combined nucleation and crystal growth in the 600°C region, it is not unreasonable to conclude that these values are essentially equal. Coupling this observation with the similar density behavior, X-ray diffraction patterns, and particle morphology, it is possible that the mechanism is essentially the same in both temperature regions.

VI. A PROPOSED MECHANISM FOR CRYSTALLIZATION
OF $K_2Mg_5Si_8O_{20}F_4$ GLASS

Considering the experimental observations discussed above, the following mechanism for crystallization of the $K_2Mg_5Si_8O_{20}F_4$ mica glass is proposed.

The amorphous material as quenched from above the melting point contains fluorine, magnesium, and potassium ions distributed throughout the silicon-oxygen network structure. The fluorine ions could occupy oxygen sites in the network structure, while the magnesium and potassium ions are most probably present in interstitial or network modifying sites.

Thermal excitation produced by heating the quenched structure to temperatures in the vicinity of 580°C could induce movement of fluorine ions from positions in the network structure to more energetically favorable positions, e.g. the positions forming the apices of octahedral sites around the magnesium ions. Such disengagement of fluorine from positions in the network structure could account for the drastic volume shrinkage, as well as the evolution of heat observed in this temperature region. The effect of fluorine content on exothermic peak position in DTA results indicates that fluorine plays an important role in determining the ease with which the transformation occurs. The function of fluorine as it moves into the ordered positions would be analogous to a nucleation catalyst, partially

forming the octahedra which then form the central portion of the synthetic mica unit cell.

Layton and Herczog⁽³⁰⁾ report that heterogeneities in a quenched glass in the $\text{Na}_2\text{O-Nb}_2\text{O}_5\text{-SiO}_2$ system are transformed to a pseudocrystalline form through thermal excitation. In this system the onset of crystallization occurs at 680°C and is very rapid; the final stage of crystallization is described as slow because of larger diffusion distances involved. A similar mechanism appears likely in the $\text{K}_2\text{Mg}_5\text{Si}_8\text{O}_{20}\text{F}_4$ glass.

Heat treatments at temperatures just above the vicinity of the 600°C region of the initial transformation provide results suggesting the development of crystalline structure is limited by certain factors. The low intensity, broad diffraction lines of these specimens - treated at temperatures below 800°C - indicates the presence of relatively small particles. Duke, et al⁽³¹⁾ observed similar diffraction lines in the early crystallization stages of a nepheline glass-ceramic body. They interpreted this as an indication of crystalline particles of less than 1000 \AA dimensions. Thus, the consistently broad, low intensity diffraction lines observed over the range of treatment temperatures from 580 to 625°C can be associated with a static crystalline particle size of less than 1000 \AA .

This limit to crystal growth could result from a relatively immobile species failing to assume its preferred crystalline site. Assuming that the silica network has

ordered during heat treatment in this 600°C region (which is indicated by X-ray diffraction patterns), and the fluorine and magnesium ions are in or near their correct lattice positions, the only remaining species would be the potassium ions. Thus higher temperatures (a more open structure) would favor the movement of potassium ions to preferred lattice sites. Since potassium ions act to bond adjacent mica layers to one another this high temperature mobility can be correlated to the change of crystal habit and development of complete crystallinity at temperatures of 900°C and above.

VII. CONCLUSIONS

An investigation of the crystallization behavior of a tetrasilicic synthetic mica glass ($K_2Mg_5Si_8O_{20}F_4$) has been conducted over a 600°C temperature range from 560 to 1150°C. The following conclusions have been extracted from data analysis:

1. The initial appearance of crystalline phase as detected by X-ray diffraction occurs after an isothermal treatment at 560°C for 9 hours.

2. Electron replication microscopy and electron scanning microscopy indicate that a change in particle morphology without a change in crystalline structure occurs between 800 and 900°C under isothermal conditions.

3. A mechanism for the transformation from amorphous to crystalline structure for the $K_2Mg_5Si_8O_{20}$ composition is proposed to be a two stage process:

- a) The development of an initial crystalline phase which rapidly attains a limiting particle size and morphology at temperatures just above 600°C, and,

- b) a more complete development of crystallinity and change of particle morphology, with no change in structure at temperatures from 900 to 1150°C.

BIBLIOGRAPHY

1. Levine, A. K., and Nathanshon, S., "Growth of Sheet Crystals of Fluorophlogopite", Amer. Cer. Soc. Bull. 45 (3) 307-311 (1966).
2. Tuzzeo, J. J., "Development of a Fluor-Mica Dielectric Using Glass-Ceramic Fabrication Methods", M.S. Thesis University of Missouri-Rolla pp. 61 (1964).
3. Schumacher, R. F., "The Dielectric Properties of Synthetic Fluor-Mica Formed by Glass-Ceramic Fabrication Techniques", M.S. Thesis University of Missouri-Rolla pp. 51 (1965).
4. Ainsworth, J. H., "The Elastic and Anelastic Constants of a Synthetic Fluor-Mica Formed by Glass-Ceramic Fabrication Techniques", M.S. Thesis University of Missouri-Rolla pp. 50 (1965).
5. Pauling, L., "The Structure of Micas and Related Minerals", Nat'l. Acad. Sci. Proc. 16 (2) 123-129 (1930).
6. Winchell, A. N., "Studies in the Mica Group - Part II", Amer. Jour. Sci. 9 (5) 415-430 (1925).
7. Skow, M. L., "Mica, A Materials Survey", U. S. Bureau of Mines IC 8125 pp. 239 (1962).
8. Seifert, F., and Schreyer, W., "Synthesis of a New Mica, $\text{KMg}_{2.5}[\text{Si}_4\text{O}_{10}]\text{D}(\text{OH})_2$ ", Amer. Mineral. 56 (4) 1114-1118 (1965).
9. Alley, J. K., and Shell, H. R., "Melting Temperatures of Fluormicas and Related Compounds", U. S. Bureau of Mines RI 598 pp. 32 (1962).
10. Hatch, R. A., Humphrey, R. A., Eitel, W., and Comeforo, "Synthetic Mica Investigations IX: Review of Progress from 1947 to 1955", U. S. Bureau of Mines RI 5337 pp. 79 (1957).
11. Hillig, W. B., "A Theoretical and Experimental Investigation of Nucleation Leading to Uniform Crystallization of Glass", Symposium on Nucleation and Crystallization in Glasses and Melts, 77-89: Amer. Cer. Soc., Columbus, Ohio, M. K. Reser Editor pp. 123 (1962).

12. Cahn, J. W., and Charles, R. J., "The Initial Stages of Phase Separation in Glasses", *Phys. Chem. Glasses* 6 (5) 181-191 (1965).
13. Stookey, S. D., and Maurer, R. D., "Catalyzed Crystallization of Glass - Theory and Practise", *Piogr. Cer. Sci.*, Vol. 2, 77-101, Pergamon Press, J. E. Burke Editor (1962).
14. Roy, R., "Phase Equilibria and the Crystallization of Glasses", Symposium on Nucleation and Crystallization in Glasses and Melts, 39-45: Amer. Cer. Soc., Columbus, Ohio, M. K. Reser Editor pp. 123 (1962).
15. Cahn, J. W., "Spinodal Decomposition", *Trans. A.I.M.E.* 242 166-180 (1968).
16. LaMer, V. K., "Nucleation in Phase Transitions", *Ind. Engr. Chem.* 44 (6) 1270-1277 (1952).
17. Emrich, B. R., "Technology of New Devitrified Ceramics - A Literature Review", Technical Documentary Report No. ML-TDR-64-203, Air Force Systems Command, Wright-Patterson Air Force Base pp. 149 (1964).
18. Chen, F. P. H., "Kinetic Studies of Crystallization of Synthetic Mica Glass", *Amer. Cer. Soc.* 46 (10) 476-484 (1963).
19. Rindone, G.E., "Further Studies of the Crystallization of a Lithium Silicate Glass", *Jour. Amer. Cer. Soc.* 45 [1] 7-12 (1962).
20. Jaccodine, R. J., "Study of Devitrification of Lithium Glass", *Jour. Amer. Cer. Soc* 44 [10] 472-475 (1961).
21. Bergeron, C. G., and Russell, C. K., "Nucleation and Growth of Lead Titanate from a Glass", *Jour. Amer. Cer. Soc.* 48 [3] 115-118 (1965).
22. Preston, E., "Crystallization Relationships of a Soda-Lime-Magnesia-Silica Glass as Used for Drawn Sheet and the Process of Devitrification", *Jour. Soc. Glass Tech.* 24 [104] 139-158 (1940).
23. Swift, H. R., "Effect of Magnesia and Alumina on Rate of Crystal Growth in Some Soda-Lime-Silica Glasses", *Jour. Amer. Cer. Soc.* 30 [6] 170-174 (1947).

24. Brown, S. D., and Ginell, H., "Partial Structure of Glass and the Reconstructive Nature of Devitrification Processes"; Symposium on Nucleation and Crystallization in Glasses and Melts, pp. 109-118: Amer. Cer. Soc., Columbus, Ohio, M. K. Reser Editor pp. 123 (1962).
25. Knight, M. A., "Glass Densities by the Settling Method", Jour. Amer. Cer. Soc. 28 (11) 297-322 (1945).
26. Tudorovskaya, N. A., and Sherstyuk, A. I., "Study of Catalyzed Crystallization by Differential Thermal Analysis", The Structure of Glass, Vol. 3, 126-128: Catalyzed Crystallization of Glass, Consultants Bureau, New York, New York, E. A. Porai-Koshits Editor (Translated from Russian) (1964).
27. Freiman, S. W., and Hench, L. L., "Kinetics of Crystallization in $\text{Li}_2\text{O-SiO}_2$ Glasses", Jour. Amer. Cer. Soc. No. 3 Fabrication Science 229-240 (October, 1965).
28. MacDowell, J. F., "Nucleation and Crystallization of Barium Silicate Glasses", Proc. Br. Cer. Soc. No. 3 Fabrication Science 229-240 (October, 1965).
29. Blau, H. H., "Trouble Shooting and Glass Research", Amer. Cer. Soc. Bull. 41 (5) 317-320 (1962).
30. Layton, M. M., and Herczog, A., "Nucleation and Crystallization of NaNbO_3 from Glasses in the $\text{Na}_2\text{O-Nb}_2\text{O}_5\text{-SiO}_2$ System", Jour. Amer. Cer. Soc. 50 (7) 369-375 (1967).
31. Duke, D. A., MacDowell, J. F., and Karstetter, B. R., "Crystallization and Chemical Strengthening of Nepheline Glass-Ceramics", Jour. Amer. Cer. Soc. 50 (2) 67-74 (1967).
32. Bergeron, C. G., Russell, C. K., and Friedberg, A. L., "Thermal Analysis of Lead Borate Glasses During Crystallization", Jour. Amer. Cer. Soc. 46 (5) 246-247 (1963).

Vita

William Henry Daniels was born March 17, 1940 in Toledo, Ohio. Upon completion of primary and secondary schooling in the public school system of Swanton, Ohio he enrolled in Ohio State University in September, 1958. He received a Bachelor of Ceramic Engineering degree from that institution in June, 1963.

Enrolling in the University of Missouri at Rolla in September, 1963, he received a Masters of Science degree in Ceramic Engineering in August, 1964. From 1964 to 1967 he continued studies as a National Science Foundation Pre-doctoral Trainee at the University of Missouri at Rolla.

He is a member of the American Ceramic Society, Keramos, National Institute of Ceramic Engineers, and American Society for Testing and Materials.